

Selective Human Estrogen Receptor Partial Agonists (ShERPAs) for Tamoxifen-Resistant Breast Cancer

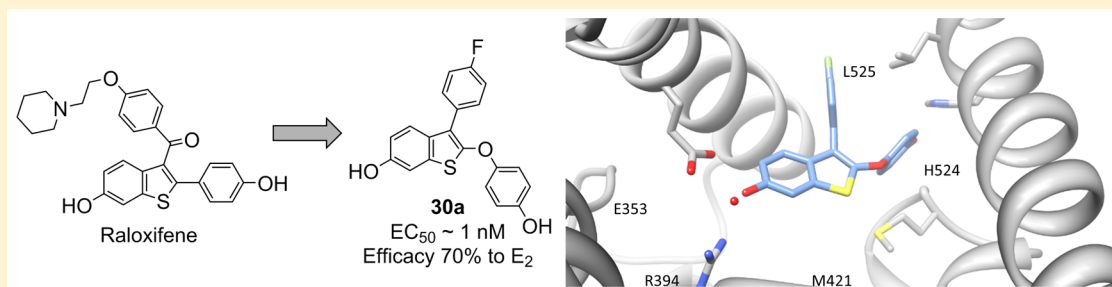
Rui Xiong,^{†,||} Hitisha K. Patel,^{†,||} Lauren M. Gutgesell,[†] Jiong Zhao,[†] Loruham Delgado-Rivera,[†] Thao N. D. Pham,[‡] Huiping Zhao,[‡] Kathryn Carlson,[§] Teresa Martin,[§] John A. Katzenellenbogen,[§] Terry W. Moore,[†] Debra A. Tonetti,[‡] and Gregory R. J. Thatcher^{*,†}

[†]Department of Medicinal Chemistry and Pharmacognosy, University of Illinois at Chicago, 833 S. Wood Street, Chicago, Illinois 60612, United States

[‡]Department of Biopharmaceutical Sciences, University of Illinois at Chicago, 833 S. Wood Street, Chicago, Illinois 60612, United States

[§]Department of Chemistry, University of Illinois, Urbana—Champaign, 600 South Mathews Avenue, Urbana, Illinois 61801, United States

S Supporting Information



ABSTRACT: Almost 70% of breast cancers are estrogen receptor α (ER α) positive. Tamoxifen, a selective estrogen receptor modulator (SERM), represents the standard of care for many patients; however, 30–50% develop resistance, underlining the need for alternative therapeutics. Paradoxically, agonists at ER α such as estradiol (E_2) have demonstrated clinical efficacy in patients with heavily treated breast cancer, although side effects in gynecological tissues are unacceptable. A drug that selectively mimics the actions of E_2 in breast cancer therapy but minimizes estrogenic effects in other tissues is a novel, therapeutic alternative. We hypothesized that a selective human estrogen receptor partial agonist (ShERPA) at ER α would provide such an agent. Novel benzothiophene derivatives with nanomolar potency in breast cancer cell cultures were designed. Several showed partial agonist activity, with potency of 0.8–76 nM, mimicking E_2 in inhibiting growth of tamoxifen-resistant breast cancer cell lines. Three ShERPAs were tested and validated in xenograft models of endocrine-independent and tamoxifen-resistant breast cancer, and in contrast to E_2 , ShERPAs did not cause significant uterine growth.

INTRODUCTION

The estrogen receptors, ER α and ER β , are transcription factors that regulate genes involved in cell proliferation, differentiation, and migration. Dysregulation of ER α signaling is associated with breast cancer development, which has made ER α an attractive drug target.^{1,2} The archetype selective estrogen receptor modulator (SERM) tamoxifen is the standard of care for many patients with ER-positive (ER+) breast cancer and is intended to antagonize the actions of estrogens at ER α in the breast, although it poses an increased risk of endometrial cancer.^{3–5} Aromatase inhibitors that block estrogen biosynthesis are presently used as an alternative to tamoxifen; however, both tamoxifen and aromatase inhibitors cause compliance problems, due to side effects such as hot flashes, arising from antiestrogenic actions in nongynecological tissues. Paradoxically, before the advent of tamoxifen as standard of care, estrogen and the full ER α agonist, diethylstilbesterol (DES), were used for the treatment of

advanced ER+ breast cancer but were discontinued due to unacceptable, adverse effects.^{6,7}

Most importantly, in about 30–50% of women undergoing tamoxifen treatment, resistance occurs, leaving these women with no alternative but cytotoxic chemotherapy.^{4,8} The cause of tamoxifen resistance and endocrine independence of ER+ breast cancer is not fully defined and may include remodeling of several cellular systems; for example, an overexpression of growth factor receptors, increased activity of downstream kinase pathways, phosphorylation of ER and its coregulators, and mutations in ER.^{9–11} The clinical benefits of estrogen or compounds with estrogenic activity have been largely forgotten or overlooked in the treatment of breast cancer,^{12,13} despite demonstrated efficacy in recent clinical trials in patients with heavily pretreated,

Received: August 14, 2015

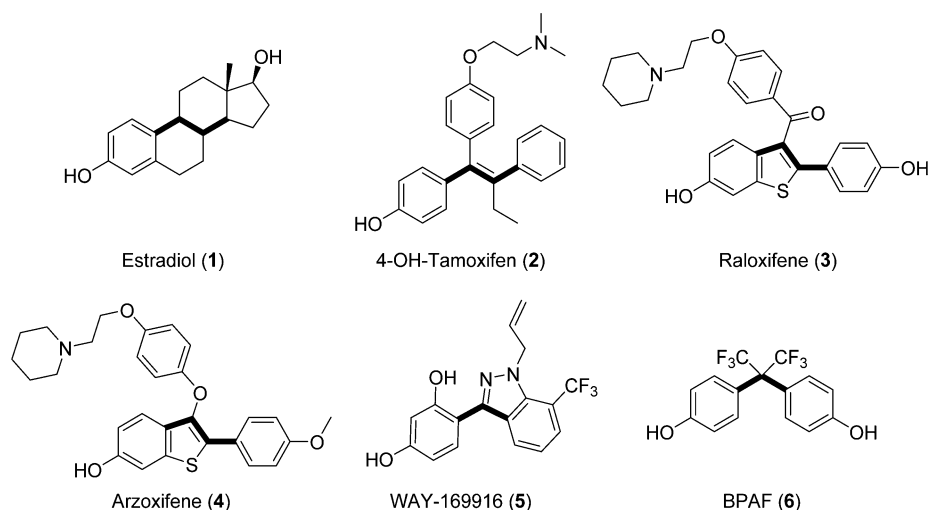


Figure 1. Structures of representative estrogen receptor ligands emphasizing the 2–4 carbon bond linking 2 phenol groups.

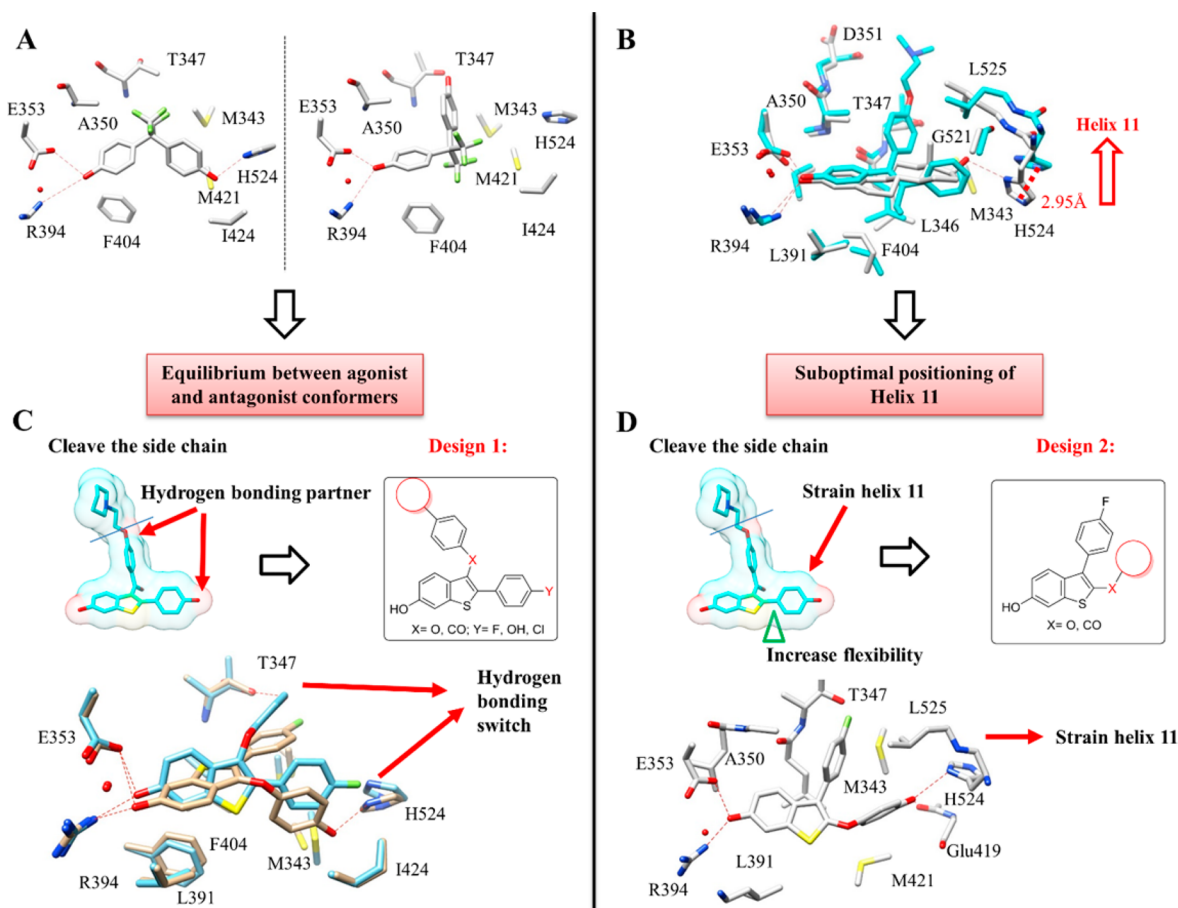
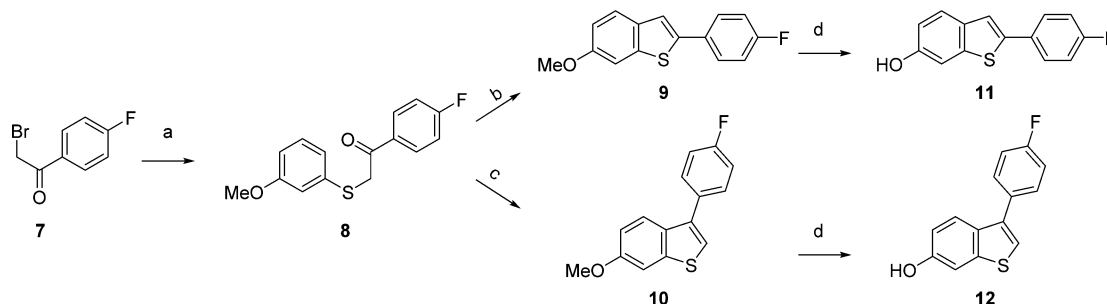


Figure 2. Design of partial agonists. (A) Crystal structure of BPAF (6) (PDB code 3UUA) bound to ER LBD shows two binding modes with hydrogen bonding switch from His-524 to Thr-347, suggestive of alternate binding modes leading to agonist and antagonist conformations that contributes to partial agonist activity. (B) Overlay of E_2 (1) and tamoxifen (2) crystal structures (PDB codes 1GWR and 3ERT) shows the movement of helix 11 (His-524 and Leu-525) that can lead to strain of helix 12, and a partial agonist conformation. (C) Truncation of the side chain of raloxifene and substitution of phenolic OH leads to design 1. Docking of ligand 19 shows two binding poses with alternate hydrogen bonding. (D) Insertion of a linker and diversifying substituents at C2 of the benzothiophene leads to design 2. Docking of ligand 30a shows the effect of the elongation of the 2-substituent compatible with a shift of helix 11.

metastatic ER+ breast cancer.^{14–16} In the present study, we sought to exploit the beneficial aspects of estrogenic compounds while minimizing the adverse effects. Selective human estrogen receptor partial agonists (ShERPAs) stand out as a novel

approach toward this goal. Ideally, these partial ER α agonists would mimic estradiol's efficacy in treating tamoxifen-resistant breast cancer while attenuating adverse effects that result from full estrogenicity.

Scheme 1. Synthesis of 2-(4-Fluorophenyl)- and 3-(4-Fluorophenyl)benzothiophene Cores^a

^aReagents and conditions: (a) KOH, EtOH/H₂O, 3-methoxythiophenol, rt, 2 h; (b) PPA, 120 °C, 3 h, 55% over two steps; (c) BF₃·OEt₂, DCM, rt, overnight, 73% over two steps; (d) BBr₃, DCM, −78 °C to rt, overnight.

SERMs are able to act as tissue-selective ER ligands because of the ability of liganded-ER to cause gene activation or silencing when complexed with coactivators or corepressors.^{17–19} However, the extensive search for clinical SERMs has been focused on compounds that display ER α antagonist activity in breast tissues and estrogenic, agonist activity in bone tissues in postmenopausal women.²⁰ The SERM, raloxifene, in clinical use for postmenopausal osteoporosis for over a decade, appears safe and noncarcinogenic and is clinically indicated for chemoprevention of invasive breast cancer. Arzoxifene, an analogue of raloxifene and a “third generation” SERM, demonstrated a favorable profile in preclinical studies,²¹ and its active metabolite is more potent than raloxifene.^{22–26} The indole SERM, bazedoxifene, was recently approved in Europe for postmenopausal osteoporosis.^{27–29} We have focused upon a deeper understanding of ER ligands based upon the benzothiophene scaffold, common to raloxifene and arzoxifene.^{30–41} Recently, we demonstrated in two different animal models of tamoxifen-resistant breast cancer that a prototype benzothiophene ShERPA caused regression of established xenografts in the absence of the uterine weight gain shown by E₂.⁴² Herein we report the design, synthesis, optimization, and characterization of potent ShERPAs with potential for treatment of endocrine-independent and tamoxifen-resistant breast cancer.

■ STRUCTURE DESIGN

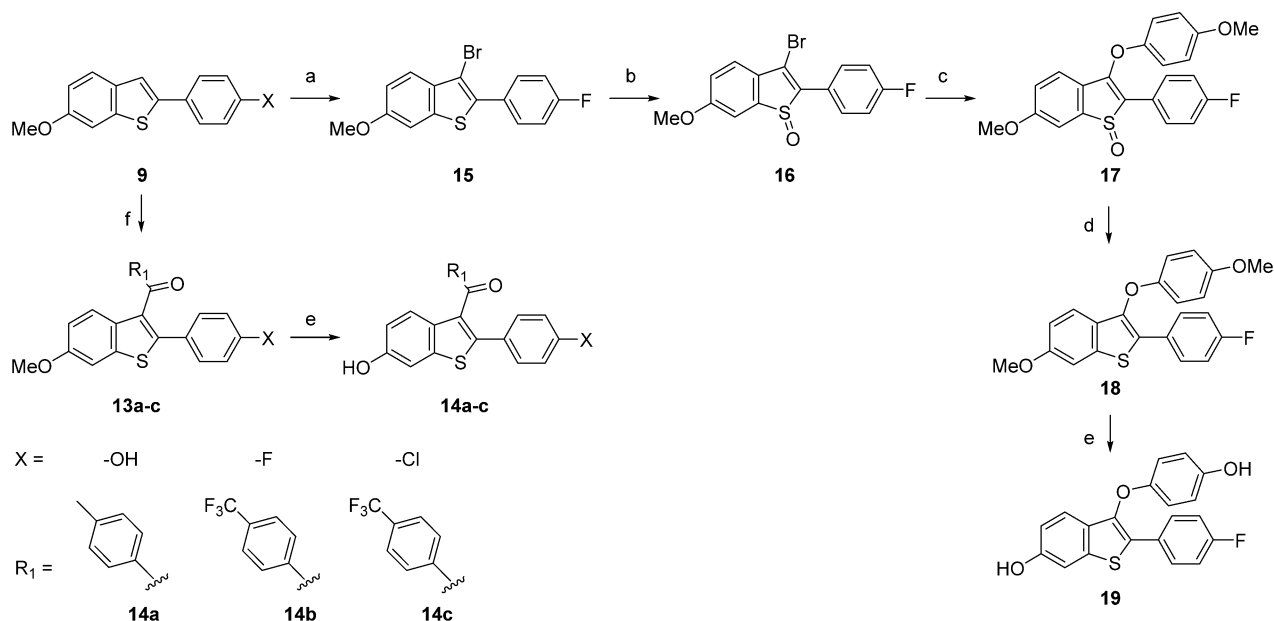
The plasticity of the ER ligand-binding domain (LBD) is reflected by the structural diversity of ER ligand scaffolds (Figure 1) and lends itself to design of novel pharmacological modulators.^{43,44} The volume of the ER ligand-binding pocket is ~450 Å³ and can accommodate ligands as small as 250 Å³ (e.g., estradiol, E₂; PDB code 1gwr) or as large as 380 Å³ (e.g., 17R-(2E-trifluoromethylphenylvinyl)-E₂; PDB code 2p15).⁴⁵ The ligand-binding domain of ER comprises 12 α helices and a β sheet. These secondary structures create an interior hydrophobic cavity forming a ligand binding site and a hydrophobic, solvent-exposed surface to which transcriptional coregulators bind.⁴⁶ In the “mousetrap” model of ER, helix 12 is closed, allowing coregulator binding (agonist mode), or open and hindering coregulator binding (antagonist mode).⁴⁶ This binary model may have limited pursuit of partial agonists at ER; however, even in this mousetrap view, a ligand that can stabilize both agonist and antagonist conformations may act as a partial agonist.

Partial estrogenic activity (defined by maximal activity significantly lower than E₂) has been reported for genistein in cell cultures; however, this submaximal activity at micromolar concentrations may be associated with the many other known

cellular targets of genistein.^{47–49} ER α partial agonist activity has also been reported for ligands in hepatocarcinoma cell lines transfected with ER or endometrial cell lines; however, these observations have not been followed up in mammary cells containing native, functional ER or to confirm pharmacological partial agonism.^{50–53} Relatively weak and partial agonist activity was reported for bisphenol AF (BPAF)⁵⁴ and WAY-169916 congeners,⁵⁵ compatible with stabilization of suboptimal conformations of ER, which might form weaker complexes with coregulators. The crystal structure with WAY-169916 (PDB code 2qzo)⁵⁶ showed a conformation structurally different from the ER α /E₂ complex due to a shift of helix 11 toward helix 12. A similar shift at helix 11 by placing a 4-methoxyphenyl group at the 11 β position of E₂ was also proposed as a potential mechanism for inducing ligand transition from an agonist to a partial agonist.⁵³ In the case of ER α /BPAF crystal structures, two conformations were revealed in the same crystal structure, with one monomer of the homodimer occupying an “antagonist” conformation and the other an “agonist” conformation. This emphasizes that ligand:ER complexes can adopt multiple stable binding modes and that these might correspond to agonist, antagonist, or partial agonist conformations (Figure 2A).⁵⁴

ER ligands commonly possess two phenol groups linked by two to four chemical bonds, with phenolic-OH separation of 11–12 Å. The central scaffold is usually planar and hydrophobic (Figure 1).⁴³ An overlay of the E₂ and tamoxifen-bound ER α structures demonstrates the large shift in the terminal residues of helix 11, caused by the tamoxifen side chain, resulting in displacement of helix 12 and antagonist activity (Figure 2B). A closer look at the structure of ER α complexed with WAY-169916 shows that the smaller shift of helix 11, repositioning His-524 and Leu-525, strains helix 12 without complete displacement. The ER α :BPAF structures show a switch from His-524 to Thr-347 as a key hydrogen bonding residue with the ligand, demonstrating a dynamic hydrogen bonding network that can accommodate diverse agonists or antagonists in various poses (Figure 2A). We hypothesized that novel ligands could maintain high affinity and potency while acting as partial agonists by exerting small shifts in helix 11 and exploiting the dynamic hydrogen bonding network for stabilization.

To develop partial agonists, we chose the benzothiophene scaffold, common to the SERMs arzoxifene and raloxifene, the latter having a superior safety profile to tamoxifen. As depicted in Figure 2C,D, the initial design step was to truncate the SERM side chain to avert complete displacement of helix 12 and to avoid a pure antagonist. A small probe library was prepared using interchange and substitution of phenolic substituents to explore the effect on activity of truncation and replacing phenolic OH.

Scheme 2. Synthesis of 2-(4-Fluorophenyl)benzothiophenes^a

^aReagents and conditions: (a) *N*-bromoacetamide, DCM/EtOH, rt, 2 h, 78%; (b) H₂O₂, TFA, DCM, 0 °C, 2 h, 75%; (c) 4-methoxyphenol, NaH, DMF, rt, 3 h, 93%; (d) LiAlH₄, THF, 0 °C, 2 h, 71%; (e) BBr₃, DCM, −78 °C to rt, overnight; (f) AlCl₃, R₁COCl, DCM, rt, 2–48 h.

We hypothesized that partial agonist activity could result from alternate binding modes, as seen in BPAF complexes, which might correspond to agonist and antagonist conformations (design 1, Figure 2C), or alternatively, from a shift in helix 11, causing strain in helix 12 and consequently suboptimal coregulator binding (design 2, Figure 2D). We inserted an ether or ketone linker at C2 intended to displace the 2-benzothiophene substituent to interact directly with the terminal residues of helix 11, causing strain in helix 12 (design 2).

CHEMISTRY

2-(4-Fluorophenyl)-6-methoxybenzo[*b*]thiophene (**9**) was prepared by the cyclization rearrangement induced by polyphosphoric acid (PPA) as reported by Jones and colleagues.⁵⁷ The regioisomer 3-(4-fluorophenyl)-6-methoxybenzo[*b*]thiophene (**10**) was synthesized with BF₃·OEt₂ in dichloromethane (Scheme 1). Arylation at C3 of benzothiophene was accomplished by direct Friedel–Crafts acylation. Coupling with the acid chloride bearing a strong electron withdrawing group, e.g., **14b**, gave multiple isomers and minor products, and a C18 reverse-phase column was used to purify the final products (Scheme 2). A trans-halogenation minor product, **14c**, was isolated from the preparation of **14b** with 3% isolated yield, possibly from a S_NAr displacement of fluoride by chloride.^{58,59} C2 benzothiophene arylation used a similar strategy with the exception of products containing strong electron withdrawing groups, which were obtained using *n*-butyllithium to generate an organic lithium salt that reacts directly with the acid chloride (Scheme 3). The synthesis of ether-linked derivatives was accomplished by adapting a reported procedure (Scheme 4).³² Bromination of the benzothiophene core with *N*-bromoacetamide provided exclusively the monobrominated product in high yield, which was activated for S_NAr reaction by oxidation to the sulfoxide under H₂O₂. Introduction of the substituted phenol was accomplished in the presence of NaH in DMF. Sulfoxide reduction was performed under LiAlH₄ in THF. Deprotection of the methyl group was achieved by BBr₃ or BF₃·SMe₂ to give the

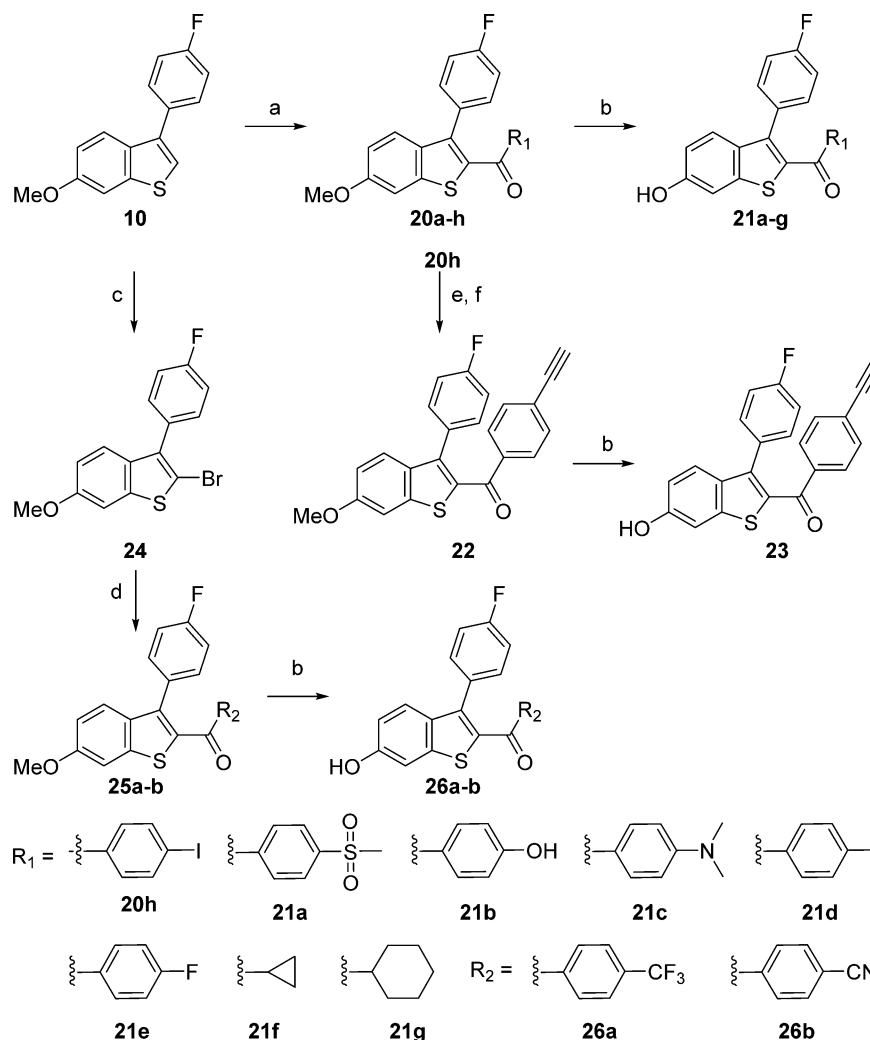
final product. Regioisomers were verified by 2D NMR, and one of the key intermediates was recrystallized for X-ray crystallography for structural confirmation (Supporting Information Figure 1).

BIOLOGICAL TESTING

Ligand affinity and estrogenic potency were evaluated, respectively, in a fluorescence polarization (FP) binding assay using full-length ERα and a cell-based assay using an estrogen response element (ERE) luciferase reporter (Table 1). Ligand affinity of selected ShERPAs was also studied by radioligand displacement (Table 2). Potency and efficacy (*E*_{max}) for ERE-luciferase activation were measured in endocrine-dependent ER+ MCF-7:ws8 cells, the response being normalized to control treated cells (0%) and E₂ (1 nM) treated cells (100%).

Pharmacological partial agonists are defined by the submaximal efficacy compared to the preferred, endogenous ligand and by antagonism of the activity of the endogenous agonist. Antagonism has rarely been tested in the literature for putative partial agonists at ER. By definition, a ShERPA must antagonize the actions of E₂ in breast cancer cell cultures in which it exerts partial agonist activity. The therapeutic rationale for exploring ShERPAs is based upon the need for an ER ligand that mimics the actions of estrogen in killing tamoxifen-resistant breast cancer cells. Therefore, the ability of these mimics to inhibit growth of endocrine-independent, tamoxifen-resistant MCF-7:5C cells, on the ninth day after treatment, was assessed by MTS assay (confirmed by DNA assay). Results were reported as cell viability relative to vehicle (100%) (Figure 3) or as inhibition of cell growth relative to vehicle (0%) and E₂ (100%) (Table 3).

The three ERα ligands for which data are depicted in Figure 3 represent examples of a full agonist (**1**), SERM antagonist (**3**), and a ShERPA (**30a**). Panel A shows ERE-luciferase response in MCF-7:ws8 cells. Panel B shows FP measured by displacement of fluorescent E₂ from ERα, and panel C shows viability of treated tamoxifen-resistant MCF-7:5C cells.

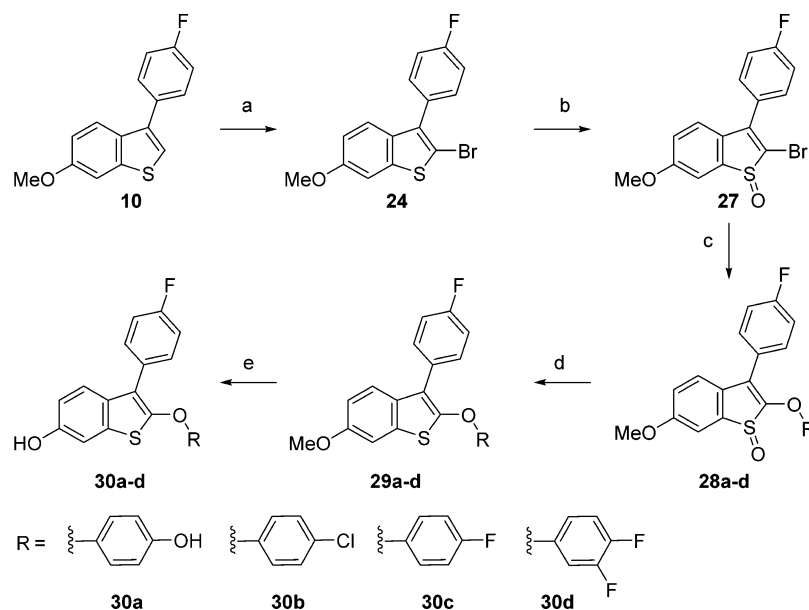
Scheme 3. Synthesis of 3-(4-Fluorophenyl)benzothiophene Compounds with a Ketone Linker^a

^aReagents and conditions: (a) AlCl_3 , R_1COCl , DCM, rt, 2–48 h; (b) BBr_3 , DCM, -78°C to rt, 4–48 h for **21a–e** and **26a,b**; $\text{BF}_3\cdot\text{SMe}_2$, DCM, 0°C to rt, 24 h for **21g** and **23**; (c) *N*-bromoacetamide, DCM/EtOH, rt, 89%, 2 h; (d) *n*-BuLi, R_2COCl , THF, -78°C to rt, 4 h; (e) Et_3N , $\text{Pd}(\text{PPh}_3)_2\text{Cl}_2$, DMF, CuI, ethynyltrimethylsilane, 4 h; (f) TBAF, THF, rt, 1 h, 50% over two steps.

ERE-Luciferase Guided Structure Optimization. A small probe library was prepared to explore side chain truncation and substitution of phenolic OH in derivatives containing the 2-phenylbenzothiophene core common to arzoxifene and raloxifene. Truncation and substitution of a methyl group at the 4'-benzoyl position switched an antagonist (raloxifene) to a potent agonist (**14a**): $\text{EC}_{50} = 2.6$ nM, efficacy (E_{max}) of ~100% (Table 1). Substitution of the phenolic OH by F in **14b** reduced potency and affinity but retained full agonist activity. Similarly, the chloro congener (**14c**) was a full agonist, and **19**, containing an ether linkage and 4'-OH replaced by F, was again a potent full agonist in MCF-7 cells: $\text{EC}_{50} = 6.2$ nM. Side chain truncation was confirmed as a route to $\text{ER}\alpha$ agonists, and replacement of phenolic OH groups was tolerated while retaining nanomolar potency. In the FP assay using ligand displacement from full length $\text{ER}\alpha$, all truncations and substitutions of raloxifene reduced relative binding affinity compared to raloxifene itself (RBA_{ral}). Even in this small conserved library of structures, correlation of affinity with potency in cell cultures was poor, driving use of the luciferase reporter assay for optimization.

Having demonstrated the simple hypothesis that side chain truncation would produce ER agonists, we proceeded to test the

proposal that insertion and elongation of the 2-benzothiophene substituent would lead to partial agonist activity. The 3-fluorophenylbenzothiophene series (**21**) yielded agonists that as in the probe library showed reduced RBA_{ral} but nanomolar, and in one case picomolar, potency for ERE activation. For example, compound **21b** with two phenolic substituents was a potent full agonist ($\text{EC}_{50} = 0.2$ nM) but with RBA_{ral} only 14% that of raloxifene. One derivative in this series, **21c**, proved to be a potent partial agonist ($\text{EC}_{50} = 30$ nM). Moreover, we were able to replace the 2-benzoyl group with sp^3 alkanoyl substituents while maintaining potency ($\text{EC}_{50} = 1\text{--}14$ nM). Within the 2-benzoyl and 2-alkanoyl benzothiophene series, 3 of 10 compounds (**21c**, **23**, **26a**) demonstrated potent partial agonist activity but with relatively low RBA_{ral} : for example, the trifluoromethyl derivative (**26a**), $E_{\text{max}} = 80\%$, $\text{EC}_{50} = 5$ nM, and the alkynyl derivative (**23**), $E_{\text{max}} = 65\%$, $\text{EC}_{50} = 5$ nM. A further series of 3-phenylbenzothiophenes with a 2-ether linkage (**30**) showed a similar pattern of activity, with relatively low RBA_{ral} , contrasting with nanomolar potency as agonists (0.8–76 nM). Directly comparing the ether- and ketone-linked series (**21b** vs **30a** and **21e** vs **30c**) revealed bis-phenolic derivatives to have relatively high potency (<1 nM) and RBA_{ral} , whereas both

Scheme 4. Synthesis of 3-(4-Fluorophenyl)benzothiophene Compounds with an Ether Linker^a

^aReagents and conditions: (a) *N*-bromoacetamide, DCM/EtOH, rt, 89%, 2 h; (b) H₂O₂, TFA, DCM, 0 °C, 2 h, 84%; (c) R₃OH, NaH, DMF, rt, 6 h for **28a**; Cs₂CO₃, DMF, 80 °C, overnight for **28b–d**; (d) LiAlH₄, THF, 0 °C, 2 h; (e) BBr₃, DCM, –78 °C to rt, 4–48 h.

bis-fluorophenyl derivatives had lower RBA_{rel} and 100-fold reduced potency (Table 1). We used G15, the inhibitor of GPER/GPR30, to test for any involvement of this extranuclear receptor in ShERPA activity. Cotreatment of cells with G15 and ShERPAs did not significantly reduce observed luciferase reporter activity (Supporting Information Figure 2).

The relatively low RBA_{rel} values obtained from the FP assay accompanied by nanomolar potency in the reporter assay led to the testing of the three ShERPAs, **23**, **26a**, and **30a**, in the classical radioligand displacement assay (Table 2). It was seen that the potent ShERPA, **30a**, exhibited 92% RBA relative to estradiol (RBA = 100%) while ShERPAs **23** and **26a** exhibited 8% and 1% RBA, respectively. While our compounds exhibit strong affinity in this assay, a lack of correlation between biochemical data and cellular response remains, confirming the use of the reporter assay as the optimal route for structure optimization.

Characterization of ShERPA Partial Agonism. All 2-phenyl and 3-phenyl benzothiophene derivatives obtained according to the design principles described in Figure 2 acted as ER α agonists. As defined by ERE-luciferase activation in ER+ breast cancer cell lines, five of these were ShERPA candidates: **21c**, **23**, **26a**, **30a**, and **30b**. When compared to full agonists, these partial agonists did not uniformly display weaker affinity (RBA_{rel}) or reduced potency for ERE activation; for example, **30a** is a partial agonist with picomolar potency and affinity for isolated ER α (RBA) not significantly different from E₂ itself. In addition to submaximal efficacy, a partial agonist should by definition antagonize the action of the endogenous agonist. The partial agonists **30a**, **23**, and **30b**, showing a range of potency (EC₅₀ = 0.8 nM, 5.3 nM, and 76.1 nM, respectively), were tested as antagonists in MCF-7:ws8 cells. Pharmacological partial agonist activity was validated by the antagonism of E₂ induced ERE activation (Figure 4).

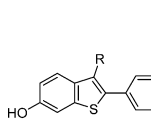
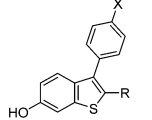
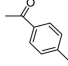
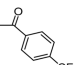
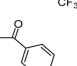
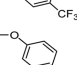
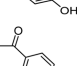
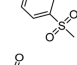
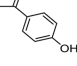
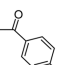
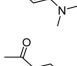
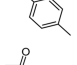
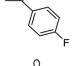
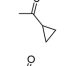
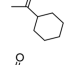
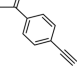
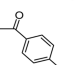
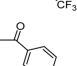
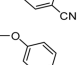
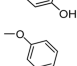
The mechanics preceding ERE activation by liganded ER include dimerization, nuclear translocation/accumulation, and binding to DNA at the ERE of a multiprotein complex containing

ER in an agonist conformation. The recruitment, assembly, and disassembly of protein complexes at DNA control transcriptional events triggered by liganded-ER.^{60–62} Recruitment of steroid receptor coregulator-3 (SRC3 or AIB1, amplified in breast cancer 1) is a key component of ER α -mediated transcription. The interaction of ER α -LBD with SRC3 coactivator is therefore a minimal predictor of phenotype, as a necessary step in the canonical nuclear ER-transactivation pathway.^{63,64} Time-resolved fluorescence (or Förster) resonance energy transfer (TR-FRET) assay of the interaction of ER α -LBD with an LxxLL-containing recognition sequence of SRC3, in the presence of E₂, has been used to identify small molecules that directly inhibit protein–protein binding.^{65,66} Ligand stabilization of the ER α /SRC3 complex is an initial and essential step in transmitting a functional, transcriptional signal and, unlike RBA measurements, will define agonist and antagonist activity. A full agonist is predicted to stabilize the ER α /SRC3 complex in a similar conformation to the E₂-bound complex, yielding a similar TR-FRET signal, whereas an antagonist in the presence of E₂ will disrupt the ER α /SRC3 complex, destroying the FRET signal.

In the TR-FRET assay, the increase of FRET signal on titration of SRC3 into solutions of E₂, **23**, or **30a** was indicative of formation and stabilization of the ER α /SRC3 complex (Figure 5A). In the presence of **23** and **30a**, the maximal FRET signal was less than 50% of that generated by the E₂-liganded ER α -LBD/SRC3 complex, compatible with **23** and **30a** acting as partial agonists. In a second TR-FRET assay, conducted in the presence of a submaximal concentration of E₂ (10 nM), titration of E₂, **23**, or **30a** led to different outcomes. While E₂ enhanced the FRET signal by increasing complexation, both **23** and **30a** reduced FRET signal, compatible with weak antagonist activity. Observations in TR-FRET, although replicating only a minimal portion of the ERE-bound ER α complex, are compatible with the designation of ShERPA activity.

Inhibition of Growth of Tamoxifen-Resistant Breast Cancer Cells. To further test the candidate ShERPAs, it was necessary to confirm their ability to mimic the actions of E₂ in

Table 1. Transcriptional Activity and Relative Binding Affinity of Benzothiophene Analogs

<div style="display: flex; justify-content: space-around; align-items: center;"> <div style="text-align: center;">  <p>11 - 19</p> </div> <div style="text-align: center;">  <p>12, 21a - 30d</p> </div> </div>					
Compounds	X	R	ERE luciferase ^a EC ₅₀ (nM)	Efficacy(% E ₂)	RBA _{ral} ^b
3			NA	0	100 ± 14.4
11	-OH	-H	NA	0	0.6 ± 0.2
12	-F	-H	NA	0	0.2 ± 0.1
14a	-OH		2.6 ± 0.4	100	3.3 ± 0.2
14b	-F		61.5 ± 14.4	100	0.9 ± 0.4
14c	-Cl		121 ± 19.2	100	1.2 ± 0.2
19	-F		6.2 ± 2.8	100	32.6 ± 2.3
21a	-F		436.2 ± 112.1	100	4.4 ± 1.3
21b	-F		0.2 ± 0.1	100	13.8 ± 0.9
21c	-F		30.6 ± 14.4	51	0.4 ± 0.1
21d	-F		717.1 ± 261.6	100	3.8 ± 1.0
21e	-F		18.5 ± 9.5	100	5.1 ± 3.7
21f	-F		13.9 ± 3.3	100	14.4 ± 5.7
21g	-F		1.0 ± 0.1	100	1.9 ± 0.3
23	-F		5.3 ± 1.7	65	2.1 ± 0.7
26a	-F		5.2 ± 1.4	85	0.5 ± 0.1
26b	-F		58.7 ± 8.6	100	0.9 ± 0.2
30a	-F		0.8 ± 0.3	60	14.2 ± 0.8
30b	-F		76.1 ± 25.1	70	0.4 ± 0.1
30c	-F		36.8 ± 4.4	100	0.4 ± 0.1
30d	-F		33.4 ± 2.5	100	0.4 ± 0.1

^aIn MCF-7:ws8 cells, estrogenic activity was measured using a luciferase reporter assay and normalized to Ctrl (0%) and E₂ 1 nM (100%). Data show the mean ± SEM determined from an average of at least three passages. NA = no activity. ^bRBA_{ral} measuring reduction in FP caused by displacement of fluorescein-E₂ from ER. Data are normalized to raloxifene binding at 100% ± SEM.

Table 2. Relative Binding Affinity of Selected ShERPAs in Radioligand Displacement Assay

compd	RBA ^a
E ₂	100
26a	1.3 ± 0.3
23	7.9 ± 0.3
30a	92.4 ± 21

^aRelative binding affinity (RBA) values, determined by radiometric assays, are expressed as $\{[(IC_{50} \text{ estradiol})/(IC_{50} \text{ compound})] \times 100\} \pm$ the range or standard deviation (RBA, estradiol = 100%).

inhibiting growth of tamoxifen-resistant MCF-7 cells. A number of tamoxifen-resistant cell lines have been created by long-term exposure to tamoxifen (T47D:A18-TAM1), long-term estrogen deprivation (MCF-7:5C), or ectopic upregulation of PKC α (T47D:A18/PKC α).^{42,67,68} These stable cell lines are characterized by endocrine independence (growth independent of estrogens) and resistance to any growth inhibitory effects of tamoxifen. Many of these lines are also characterized by a paradoxical inhibition of cell proliferation on treatment by E₂ at nanomolar concentrations. In the case of MCF-7:5C cell cultures, treatment with E₂ causes a significant reduction in cell viability measured at 9 days. E₂ reduced cell viability by approximately 60% compared to vehicle control (Figure 3C). Inhibition of cell growth relative to vehicle (0%) and to E₂ (100%) was measured for the candidate selective estrogen mimics (SEMs) and ShERPAs (Table 3). For compounds 14a,b, 21b–g, and 30a at ≤ 100 nM, the percent of growth inhibition

was equivalent or superior to the maximum inhibition observed after treatment with E₂. Compound 21b gave 100% inhibition at 1 nM, and both 21g and 30a gave 100% inhibition at 10 nM. Of the candidate ShERPAs, only one did not show efficacy comparable to E₂ in inhibition of MCF-7:5C cell growth. It is important to emphasize that inhibition of growth of MCF-7:5C cells is not caused by any general cytotoxicity of SEMs and ShERPAs. This was clearly demonstrated in the parent estrogen-responsive MCF-7:ws8 cells, in which all compounds (100 nM and 1 μ M) supported growth at a level higher than DMSO control (data not shown).

Regression of Tamoxifen-Resistant Xenografts Uncoupled from Uterine Growth. We have previously reported that treatment with ShERPA, 30a, resulted in dramatic regression in the two tamoxifen-resistant breast cancer xenograft models, T47D:A18/PKC α and T47D:A18-TAM1, comparable to that observed on treatment with E₂.⁴² The efficacy of ShERPAs 23 and 26a was evaluated in the T47D:A18/PKC α model of tamoxifen resistance. The tumor xenografts were allowed to establish for 12 weeks prior to treatment. Although dose optimization was not carried out, at the single dose studied, the tumor size was shown to reduce rapidly on ShERPA treatment and within 2 weeks to shrink to half the size of control tumors (Figure 6A). Adverse estrogenic effects in gynecological tissues provided the rationale for development of ShERPAs. Estrogens are known uterotrophic agents, and even tamoxifen shows tissue-selective agonist activity in the uterus. In the T47D:A18/PKC α xenograft study, tumor regression induced by

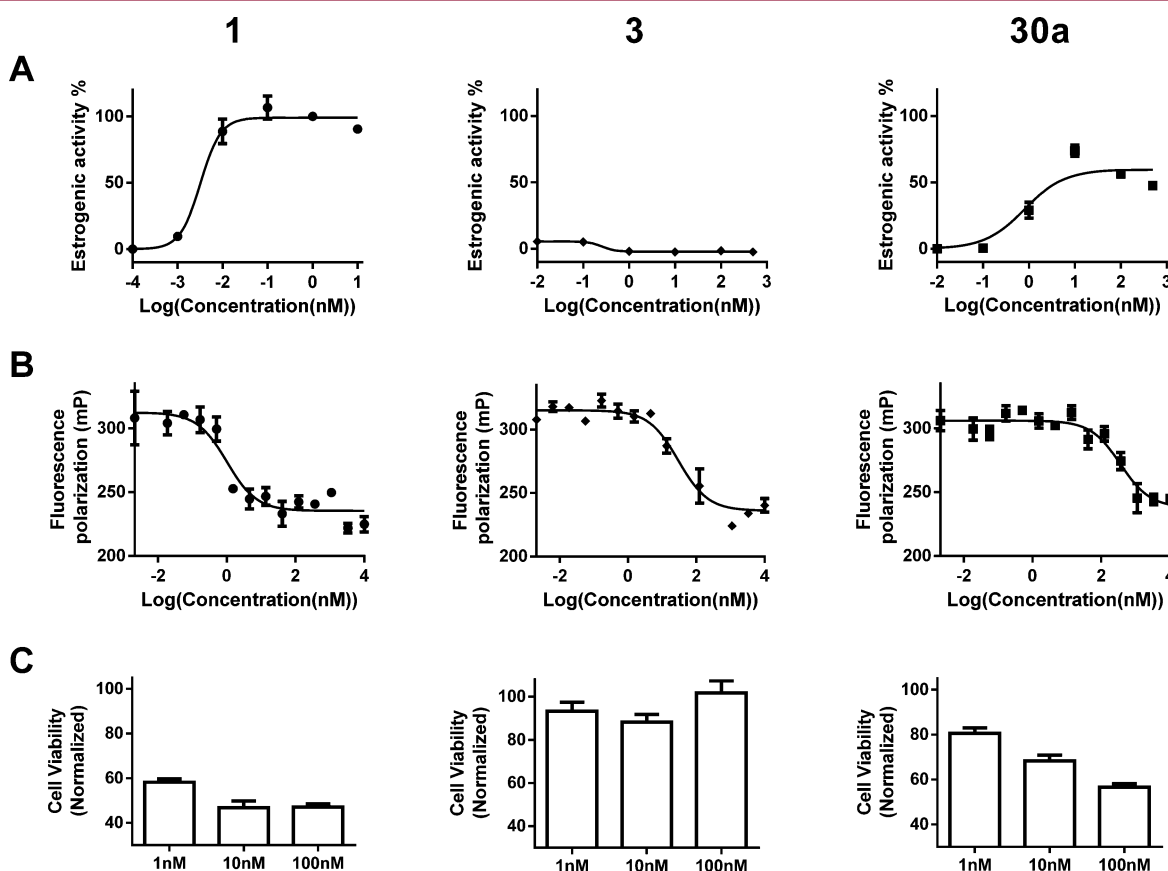


Figure 3. Profiling ER α ligands: endogenous agonist E₂ (1); SERM antagonist raloxifene (3); benzothioophene partial agonist (ShERPA) (30a). (A) Activation of ERE (estrogen response element) in MCF-7:ws8 cells. (B) RBA_{rel} from FP assay of displacement of fluorescent-E₂ from ER α . (C) Cell viability of tamoxifen-resistant MCF-7:5C breast cancer cells 9 days after drug treatment, normalized to vehicle (100%). Data show the mean and SEM.

Table 3. Cell Viability of MCF-7:5C Cells Treated with E₂ and Test Compounds

11 - 19 21a - 30d

Compounds	X	R	Inhibition of cell growth relative to E ₂ % ^a		
			1 nM	10 nM	100 nM
3			NA	NA	NA
14a	-OH		11.5 ± 4.0	60.2 ± 2.7	109.0 ± 1.4
14b	-F		55.6 ± 3.5	69.7 ± 3.6	108.0 ± 2.6
14c	-Cl		NA	NA	NA
19	-F		NA	NA	NA
21a	-F		NA	NA	18.9 ± 2.8
21b	-F		95.4 ± 2.7	99.8 ± 2.8	100.0 ± 2.1
21c	-F		4.1 ± 3.6	15.1 ± 3.1	110.9 ± 4.6
21d	-F		13.3 ± 3.8	7.4 ± 4.8	110.0 ± 4.6
21e	-F		NA	32.4 ± 5.9	131.0 ± 2.3
21f	-F		NA	79.6 ± 3.9	146.0 ± 4.5
21g	-F		21.4 ± 3.7	134.0 ± 4.2	147 ± 5.4
23	-F		31.4 ± 2.9	79.9 ± 3.1	85.6 ± 1.9
26a	-F		NA	15.4 ± 1.7	88.6 ± 2.1
26b	-F		2.0 ± 2.3	0.9 ± 2.1	64.2 ± 5.0
30a	-F		50.6 ± 3.3	104.0 ± 1.0	123.0 ± 1.7
30b	-F		NA	NA	30.7 ± 4.9
30c	-F		NA	NA	86.6 ± 8.7
30d	-F		NA	NA	84.6 ± 5.3

^aCell death percentage was normalized to control (0%) and E₂ (100%) assessed in a 9-day cell viability assay with drug treatments renewed every 3 days. Data represented as mean ± SEM are an average of at least three cell passages (triplicates in each passage).

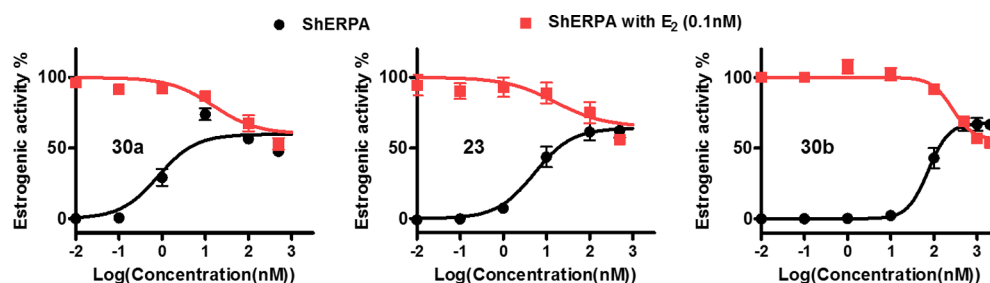


Figure 4. Partial agonist activity of three ShERPAs (30a, 23, and 30b) assessed by activation of ERE (estrogen response element) in MCF-7:ws8 cells (normalized to 0.1 nM E_2 = 100%) using a luciferase assay after treatment for 18 h. The antagonist action of these ShERPAs was assessed in the presence of 0.1 nM E_2 , and a dose dependent reduction in E_2 luciferase activity is seen with increasing concentrations of ShERPAs (100–500 nM). Data show the mean and SEM from at least three cell passages.

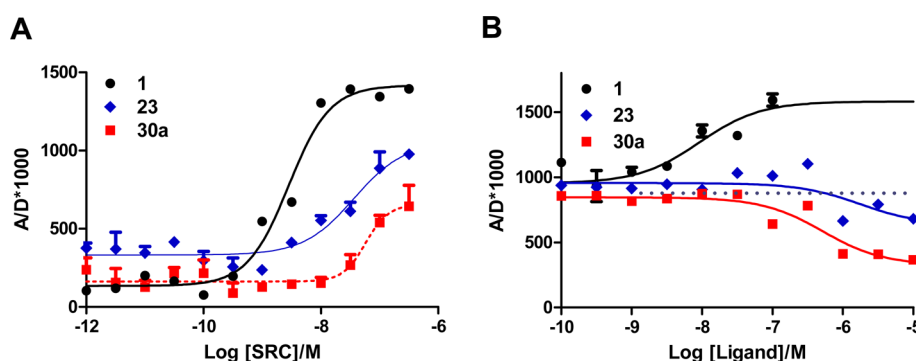


Figure 5. (A) Agonist mediated recruitment of $ER\alpha$ coactivator (SRC3). Estradiol (1) induces an increase in FRET readout with increasing concentrations of SRC3. ShERPAs 23 and 30a also show an increase in FRET signal with increasing concentration of SRC3, but maximal activation is less than 50% of E_2 . (B) Increasing concentrations of ShERPAs 23 and 30a decrease the FRET signal induced by 10 nM E_2 , attributed to the antagonist action of these molecules. The FRET signal is amplified in the presence of increasing concentrations of added E_2 (1) as is expected of an agonist. Data show the mean and SEM.

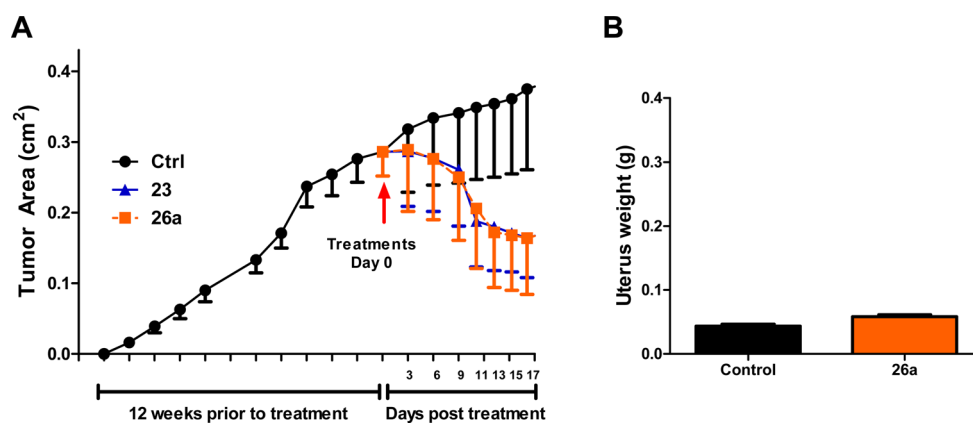


Figure 6. (A) T47D:A18/PKC α tumors were established as described in the [Experimental Section](#). Tumors were grown to an average size of 0.3 cm². Mice were then randomized into three treatment groups: Ctrl ($n = 4$), 23 and 26a ($n = 6$). Administration of drug was by oral gavage daily (100 mg/kg). Within 2 weeks of treatment, a regression of established tumors was observed, while control tumors continued to grow. (B) Measured uterine weight (g) of Ctrl ($n = 4$) and 26a ($n = 6$) treatment groups showed no significant difference, suggesting an improved side effect profile. Data show the mean and SEM.

30a was not accompanied by a significant increase in uterine weight, in contrast to E_2 .⁴² Uterine weight was measured in the xenograft study of 26a, presented herein, again showing no significant increase in uterine weight compared to vehicle control mice (Figure 6B). It is tempting to link the lack of uterotrophic activity of ShERPAs in these studies with partial agonist, submaximal efficacy at $ER\alpha$ in uterine tissues. This hypothesis cannot be confirmed in vitro because there is no cell-based model that reliably reproduces the uterotrophic actions of ER ligands.

However, these observations do predict a reduced side effect profile for ShERPAs relative to full estrogens.

DISCUSSION

The “classic” genomic actions of $ER\alpha$ as a nuclear receptor and transcription factor have dominated thinking on the role of estrogen in cancer. $ER\alpha$ is thought to mediate differentiation, apoptosis, and proliferation in normal mammary epithelial cells; however, in malignant tissues, a shift to proliferation contributes

to progression. Paradoxically, in a variety of mammary cell lines that have developed tamoxifen resistance, the proliferative phenotype of estrogen switches to an antiproliferative and apoptotic phenotype, compatible with the clinical efficacy of E_2 in advanced ER+ breast cancer.^{14–16,42}

Array and CHIP technologies have allowed mapping of ER to regulatory regions of activated and repressed target genes, showing that liganded-ER may cause gene activation or silencing, dependent on ligand stabilization of multiprotein transcriptional complexes, containing either coactivators or corepressors.^{17–19} ER α ligands may therefore act in a cell and tissue selective manner as exemplified by the SERMs raloxifene and tamoxifen: both SERMs act as estrogen antagonists in breast tissue but as estrogen agonists in the bone tissue of postmenopausal women. In contrast to SERM antagonists, the goal of this study was to design agonists at ER α , selectively to mimic the actions of estrogen in ER+ tamoxifen-resistant breast cancer.^{69,70} This goal was founded on the clinical efficacy of E_2 and the ER agonist, DES, in advanced ER+ breast cancer.^{6,7} Cognizant of the unacceptable side effects of these estrogens, it was hypothesized that ShERPAs, as partial agonists, would minimize excessive estrogenic activity in other gynecological tissues, for example, the uterus.

The design of ShERPAs, utilizing the benzothiophene core of raloxifene, was guided by structural information from published ER α -LBD crystal structures. In tamoxifen-resistant breast cancer cells, a ShERPA must stabilize ER α as part of a multiprotein complex at ERE, mimicking E_2 ; however, partial agonism is desired to minimize full estrogenic side effects. Hypothetically, an ER α ligand that yields a less stable multiprotein complex than the E_2 -bound complex, or a ligand that stabilizes both activated and silenced complexes would produce partial agonist activity. Such ligands are predicted to have lower potency than E_2 itself; however, potency similar to raloxifene should be achievable. The ShERPA ligands discovered in this study were profiled as pharmacological partial agonists with potency for ERE activation of 0.8–76 nM. Neither RBA_{rel} nor RBA for isolated ER α correlated with potency in cell cultures. Various studies have made similar observations on the discordance between biochemical affinity and potency in cell cultures,^{66,71–73} and alternative methodologies have been proposed.⁷⁴ Poor correlation was observed between RBA and growth inhibition in MCF-7 cells for a series of raloxifene analogues with similar RBAs but up to 100-fold differences in potency in cell cultures.⁷¹ A lack of correlation between binding affinities (RBA) and both potency for coactivator recruitment and cellular ERE-reporter activation was also apparent from a study of ER α ligands commonly used as chemical probes.⁶⁶ This is compatible with the thermodynamics of ligand binding to ER α in a multiprotein complex being influenced by other binding partners in that complex.

ShERPAs were effective in killing tamoxifen-resistant breast cancer cells in culture. Three ShERPAs were further validated in tamoxifen-resistant xenograft models; these mice show no significant increase in uterine weight, a key side effect of estrogen treatment.⁴² It would be unsafe without further research to assign these observations entirely to the partial agonist activity of ShERPAs; for example, the involvement of extranuclear ER and ER β needs to be considered. Nevertheless, we have demonstrated that potent, partial agonists at ER α can be created and that these ShERPAs have activity in vivo that is of potential therapeutic benefit in treatment of a subset of ER+ breast cancers.

■ EXPERIMENTAL SECTION

Cell Lines and Culture Conditions. MCF-7:ws8 cells were obtained from American Type Culture Collection (Manassas, VA). MCF-7:ws8 cells were cultured in phenol red containing RPMI 1640 medium supplemented with 10% fetal bovine serum, 1% Glutamax, 1% nonessential amino acids, insulin (10 μ g/mL), 1% antibiotic–antimycotic, and 5% CO₂ at 37 °C. Treatment medium was prepared by supplementing phenol red free RPMI 1640 medium with charcoal-dextran treated fetal bovine serum, while other supplements remained the same. MCF-7:5C cells were a gift from Dr. Tonetti's lab. These cells served as a tamoxifen resistance model and were obtained by long-term estrogen deprivation of MCF-7:ws8 cells. These cells were maintained in phenol-red free RPMI 1640 medium supplemented with 10% charcoal-dextran treated fetal bovine serum, 1% Glutamax, 1% nonessential amino acids, insulin (10 μ g/mL), 1% antibiotic–antimycotic, and 5% CO₂ at 37 °C.

ER Binding Studies. The ligand binding studies for test compounds to full length ER were performed using a PolarScreen nuclear receptor competitor assay (Invitrogen, Carlsbad, CA) according to the manufacturer's instructions. Briefly, serial dilutions of test compounds were performed using a Biomek 3000 Laboratory Automation Workstation in a 384 deep well polypropylene block. This served as the 100 \times serial dilution plate of all test compounds in DMSO where dilutions of test compounds were 100 \times the final concentration. The 2 \times dilution plate was prepared by adding 2 μ L of the stocks from the 100 \times plate to 98 μ L of assay buffer and mixed well. The final assay plate was prepared by adding 10 μ L of 2 \times stocks to 10 μ L of ER + fluorescein-labeled E_2 (final concentration of ER = 25 nM, fluorescein-labeled E_2 = 4.5 nM) and mixing well. The plate was then incubated for 2 h in the dark, and fluorescence polarization was measured on a SynergyH4 hybrid multimode microplate reader (Biotek). The fluorescence polarization was computed by measuring parallel and perpendicular polarizations at an excitation wavelength of 485 nm and an emission wavelength of 535 nm. IC₅₀ values were computed for unlabeled E_2 , raloxifene, and test compounds, and the relative binding affinities were computed using the following formula: $RBA_{rel} = [(IC_{50} \text{ of raloxifene}) / (IC_{50} \text{ of test compounds})] \times 100$. Relative binding affinities of **23**, **26a**, **30a** were also determined by a competitive radiometric binding assay with 2 nM [³H]estradiol as tracer (PerkinElmer, Waltham, MA) and full-length purified human ER α (Pan Vera/Invitrogen, Carlsbad, CA), as described previously.^{75,76} The RBA values were determined using the following equation: $[(IC_{50} \text{ estradiol}) / (IC_{50} \text{ compound})] \times 100$.

Induction of Estrogen Response Elements in MCF-7 Cells. Activation of ER α signaling by test compounds was measured using MCF-7:ws8 cells which were kept in stripped medium 3 days prior to treatment. Cells were plated at a density of 6×10^5 cells/well in 12-well plates and were transfected with 3 μ g of the pERE-luciferase plasmid, which contains three copies of the *Xenopus laevis* vitellogenin A2 ERE upstream of firefly luciferase. To normalize for cell viability and transfection efficiency, 1 μ g of pRL-TK plasmid (Promega, Madison, WI) containing a cDNA encoding *Renilla* luciferase was cotransfected along with ERE plasmid. Transfection was performed for 6 h using the Lipofectamine 2000 transfection reagent (Invitrogen) in Opti-MEM medium according to the manufacturer's instructions. Cells were treated with test compounds after 6 h, and the luciferase activity was measured in cell lysates after 18 h of treatment using the dual luciferase assay system (Promega) with FLUOstar OPTIMA (BMG LABTECH, Durham, NC). Antiestrogenic activity of ShERPAs was studied by cotreating with 0.1 nM E_2 to observe inhibition of E_2 response. Data are represented as an average of three passages reported as the relative luciferase percentage with 1 nM E_2 treatment set as 100% and control treated cells as 0%. The initial luciferase activity values were calculated by dividing the firefly luciferase (ERE) reading by the *Renilla* luciferase (pRL-TK) reading.

TR-FRET. FRET assay buffers (A and B) were prepared as previously reported.⁶⁶ In the SRC3 titration assay, the 3 \times concentrations of fluorescein-labeled SRC3 (5 μ L) prepared in buffer A was added to a 96-well black microplate containing premixed streptavidin–terbium (SA-Tb) and biotinylated ER α LBD (5 μ L). This was followed by the

addition of 3× concentration of ligands **1**, **23**, and **30a** (5 μ L) prepared in buffer B. The final 15 μ L assay volume contained 1 nM ER α LBD, 20 μ M ligand, and 0.25 nM SA-Tb. Assay solutions were mixed and incubated for 1 h at room temperature in the dark before being measured for TR-FRET. Parallel incubations without the biotinylated ER α LBD were performed to correct for diffusion-enhanced FRET and to correct for nonspecific binding. The background was subtracted from the total FRET values obtained from the test samples and plotted against log SRC3 concentrations. In the ligand titration assay, serial dilutions of **1**, **23**, and **30a** were added to premixed 0.25 nM streptavidin–terbium, 1 nM ER α LBD, 100 nM fluorescein-labeled SRC3, and 10 nM E₂. The plate was mixed and incubated in the dark for 1 h before measurement of the FRET signal. The donor SA-Tb was excited at 340/80 nm, and emissions from the donor and the acceptor fluorescein were monitored at 495/20 and 520/25 nm, respectively, with a 100 μ s delay. TR-FRET was measured on a Wallac Victor II plate reader (Molecular Devices, Sunnyvale, CA).

Cell Viability Assays. MCF-7:5C tamoxifen resistant cells were plated overnight at a density of 5000 cells/well. Cells were then treated with either E₂ or test compounds at 1, 10, and 100 nM. Treatments were renewed every 3 days, and the cell viability was tested at day 9 using a CellTiter 96 AQueous One solution cell proliferation assay (MTS). The absorbance was measured at 490 nm using a SynergyH4 hybrid multimode microplate reader (Biotek), and cell viability was normalized to control (DMSO) treated cells at 100%. Data are an average of at least triplicates from three different passages. The cell toxicity in MCF-7:5C was corroborated with a second cell viability DNA content assay. Briefly, cells were plated in 96-well plates at a density of 5000 cells/well and treated with test compounds for 6 days and then frozen in dH₂O for 24 h. Cells were then lysed with TNE buffer (100 μ L/well) containing 50 mL of TE buffer, 1 M NaCl, and 100 μ L of Hoechst DNA stain. The fluorescence was then measured at an excitation wavelength of 355 nm and emission wavelength of 460 nm using the SynergyH4 hybrid mode microplate reader (Biotek). MCF-7:ws8 cells were stripped 3 days prior to plating a density of 5000 cells/well in 96-well plates and allowed to attach overnight. Cells were then treated with DMSO, E₂ (1 nM), and test compounds (100 nM) for 3 days. Cell viability was measured using an MTT assay. Briefly, MTT powder was dissolved in PBS (5 mg/mL stock solution) and was added to cell medium to a final concentration of 0.5 mg/mL. The medium was removed after incubation, and 100 μ L of DMSO was added to each well. After shaking, the absorbance of the plate was measured at 570 nm using the SynergyH4 hybrid mode microplate reader (Biotek), and cell viability was normalized to control at 100%.

Animal Experiments. T47D:A18/PKCa tumors were established as previously described.⁷⁷ **23** and **26a** were administered per os at a dose of 100 mg/kg daily for 2 weeks in a formulation of 0.1% Tween 80, 10% PEG400, and 0.5% CMC solution. Drinking water was replaced with a hydrogel suspension of drugs at a concentration of 0.25 mg/mL to maintain continuous drug exposure. Tumor cross-sectional area was determined weekly using vernier calipers and calculated using the formula (length/2) \times (width/2) \times π . Mean tumor area was plotted against time (in weeks) to monitor tumor growth. The mice were sacrificed by CO₂ inhalation and cervical dislocation, and tumors and uteri were excised, cleaned of connective tissue, and immediately weighed. The Animal Care and Use Committee of UIC approved all of the procedures involving animals.

General. All chemicals and solvents were purchased from Sigma-Aldrich, Fisher Scientific, or Matrix Scientific and were used without further purification. Synthetic intermediates were purified by Biotage flash chromatography on 230–400 mesh silica gel. ¹H and ¹³C NMR spectra were recorded on Bruker DPX-400 or AVANCE-400 spectrometer at 400 and 100 MHz, respectively. NMR chemical shifts were reported in δ (ppm) using residual solvent peaks as standard (CDCl₃, 7.26 ppm (¹H), 77.16 ppm (¹³C); CD₃OD, 3.31 ppm (¹H), 49.00 ppm (¹³C); DMSO-*d*₆, 2.50 ppm (¹H), 39.52 ppm (¹³C); acetone-*d*₆, 2.05 ppm (¹H), 29.84 ppm (¹³C)). Data are reported as follows: chemical shift, multiplicity (s = singlet, d = doublet, dd = doublet of doublet, t = triplet, q = quartet, br = broad, m = multiplet, abq = ab quartet), number of protons, and coupling constants. Low-resolution

(LR) mass spectra were acquired on an Agilent 6300 ion-trap LC–MS instrument. High resolution mass spectral data were collected in-house using a Shimadzu IT-TOF. All compounds submitted for biological testing were confirmed to be $\geq 95\%$ pure by analytical HPLC. Synthetic procedures, spectral data, and HRMS for final compounds and novel intermediates are described below.

3-(4-Fluorophenyl)-6-methoxybenzo[b]thiophene (10). Methoxybenzenethiol (65 g, 7.1 mmol) was added to a round-bottom flask charged with a freshly prepared solution containing 300 mL of ethanol, 100 mL of water, and 30 g of KOH (538 mmol). The solution was cooled in an ice–water bath, and a solution of 2-bromo-1-(4-fluorophenyl)ethanone (100 g, 461 mmol) in 100 mL of ethyl acetate was slowly added. The reaction mixture was monitored by TLC until the finish. The solvents were evaporated under reduced pressure, and the residue mixture was partitioned between water and ethyl acetate. The combined organic phase was washed with brine and dried by Na₂SO₄ to give 120 g of 1-(4-fluorophenyl)-2-(3-methoxyphenylsulfanyl)ethanone, which was used in the next step without further purification. BF₃·OEt₂ was slowly added to a flask charged with 1-(4-fluorophenyl)-2-(3-methoxyphenylsulfanyl)ethanone (120 g) under argon atmosphere in an ice bath. The reaction mixture was stirred until starting material was consumed as monitored by TLC. The reaction mixture was poured into saturated NaHCO₃/ice–water, stirred 30 min, and extracted with dichloromethane. The crude product was purified by silica gel chromatography (5% dichloromethane in hexane). The combined fractions from the column were concentrated and recrystallized to give 75 g of pale yellow solid with a 54% yield over the two steps. ¹H NMR (400 MHz, CDCl₃) δ 7.71 (d, *J* = 8.9 Hz, 1H), 7.56–7.48 (m, 2H), 7.38 (d, *J* = 2.2 Hz, 1H), 7.21–7.12 (m, 3H), 7.02 (dd, *J* = 8.9, 2.2 Hz, 1H), 3.90 (s, 3H). ¹³C NMR (100 MHz, CDCl₃) δ 162.49 (d, *J*_{C–F} = 246.7 Hz), 157.73, 142.24, 136.79, 132.34, 132.14, 130.30 (d, *J*_{C–F} = 8.0 Hz), 123.47, 120.85, 115.78 (d, *J*_{C–F} = 21.4 Hz), 114.70, 105.42, 55.80.

2-(4-Fluorophenyl)benzo[b]thiophen-6-ol (11). 2-(4-Fluorophenyl)-6-methoxybenzo[b]thiophene (**9**)³² (4.8 g, 18.6 mmol) was dissolved in 100 mL of anhydrous dichloromethane and cooled to –78 °C under a dry ice–acetone bath. BBr₃ (1.0 M in CH₂Cl₂, 55 mL, 55 mmol) was added dropwise to this solution. The reaction mixture was stirred until starting material was consumed as monitored by TLC and then quenched by saturated NaHCO₃/ice–water. The solution was extracted with ethyl acetate and washed with brine. The organic extracts were combined, dried over anhydrous Na₂SO₄, concentrated in vacuum, and then purified by flash chromatography (5–30% ethyl acetate in hexane) to give 3.3 g of white solid (yield, 73%). ¹H NMR (400 MHz, CD₃OD) δ 7.72–7.65 (m, 2H), 7.60 (d, *J* = 8.6 Hz, 1H), 7.47 (s, 1H), 7.20 (d, *J* = 2.0 Hz, 1H), 7.14 (t, *J* = 8.8 Hz, 2H), 6.86 (dd, *J* = 8.6, 2.2 Hz, 1H). ¹³C NMR (100 MHz, CD₃OD) δ 163.81 (d, *J*_{C–F} = 246.1 Hz), 156.52, 142.33, 140.46, 135.45, 132.45, 128.77 (d, *J*_{C–F} = 8.1 Hz), 125.39, 120.41, 116.74 (d, *J*_{C–F} = 22.1 Hz), 115.73, 108.05. ESI-HRMS (*m/z*): [M – H][–] calcd for C₁₄H₈FOS, 243.0280; observed, 243.0289.

3-(4-Fluorophenyl)benzo[b]thiophen-6-ol (12). This compound was prepared using similar method as **11** and gave 780 mg of white solid (yield, 82%). ¹H NMR (400 MHz, CD₃OD) δ 7.59 (d, *J* = 8.8 Hz, 1H), 7.47 (dd, *J* = 8.6, 5.5 Hz, 2H), 7.28 (d, *J* = 2.2 Hz, 1H), 7.15–7.10 (m, 3H), 6.90 (dd, *J* = 8.8, 2.2 Hz, 1H). ¹³C NMR (100 MHz, CD₃OD) δ 163.58 (d, *J*_{C–F} = 245.1 Hz), 156.35, 143.61, 137.62, 133.77 (d, *J*_{C–F} = 3.3 Hz), 132.32, 131.23 (d, *J*_{C–F} = 8.0 Hz), 124.15, 121.15, 116.39 (d, *J*_{C–F} = 21.6 Hz), 115.54, 108.64. ESI-HRMS (*m/z*): [M – H][–] calcd for C₁₄H₈FOS, 243.0280; observed, 243.0276.

(2-(4-Fluorophenyl)-6-methoxybenzo[b]thiophen-3-yl)(4-(trifluoromethyl)phenyl)methanone (13b). To an oven-dried flask charged with 2-(4-fluorophenyl)-6-methoxybenzo[b]thiophene (258 mg, 1 mmol) and 4-(trifluoromethyl)benzoyl chloride (250 mg, 1.2 mmol) in 10 mL of dichloromethane, AlCl₃ (400 mg, 3 mmol) was added in three portions over 10 min. The mixture was stirred until the starting material was consumed and then poured into ice–water. The layers were separated, and the aqueous layer was extracted three times with dichloromethane. The organic layers were combined, washed by brine, and dried over Na₂SO₄. The crude product was purified by silica gel chromatography (1–10% ethyl acetate in hexane) to give 160 mg of yellow solid (yield, 37%). ¹H NMR (400 MHz, CDCl₃) δ 7.81 (d, *J* = 8.1

Hz, 2H), 7.68 (d, J = 8.9 Hz, 1H), 7.51 (d, J = 8.1 Hz, 2H), 7.35–7.26 (m, 3H), 7.04 (dd, J = 9.0, 2.4 Hz, 1H), 6.90 (t, J = 8.6 Hz, 2H), 3.91 (s, 3H). ^{13}C NMR (100 MHz, CDCl_3) δ 192.87, 163.07 (d, $J_{\text{C-F}}$ = 250.5 Hz), 158.30, 144.42, 140.47, 134.40 (q, $J_{\text{C-F}}$ = 32.6 Hz), 133.43, 131.25 (d, $J_{\text{C-F}}$ = 8.4 Hz), 130.72, 130.18, 129.43 (d, $J_{\text{C-F}}$ = 3.5 Hz), 125.46 (q, $J_{\text{C-F}}$ = 3.7 Hz), 124.55, 123.60 (q, $J_{\text{C-F}}$ = 272.9 Hz), 116.02, 115.70 (d, $J_{\text{C-F}}$ = 20.7 Hz), 104.65, 55.82.

(2-(4-Fluorophenyl)-6-hydroxybenzo[*b*]thiophen-3-yl)(4-(trifluoromethyl)phenyl)methanone (14b). This compound was prepared by a procedure identical with the preparation of **11** except a C18 reverse phase column was used to get the pure compound (2.5 g, yield 61%). ^1H NMR (400 MHz, CD_3OD) δ 7.77 (d, J = 8.1 Hz, 2H), 7.65 (d, J = 8.8 Hz, 1H), 7.57–7.49 (m, 2H), 7.32–7.28 (m, 3H), 6.97–6.86 (m, 3H). ^{13}C NMR (100 MHz, CD_3OD) δ 194.20, 164.30 (d, $J_{\text{C-F}}$ = 248.8 Hz), 157.41, 145.51, 142.29, 141.84, 134.95 (q, $J_{\text{C-F}}$ = 32.5 Hz), 133.65, 132.56 (d, $J_{\text{C-F}}$ = 8.5 Hz), 131.85, 131.29, 130.97 (d, $J_{\text{C-F}}$ = 3.4 Hz), 126.36 (q, $J_{\text{C-F}}$ = 3.8 Hz), 125.45, 125.02 (q, $J_{\text{C-F}}$ = 272 Hz), 116.67, 116.54 (d, $J_{\text{C-F}}$ = 22.3 Hz), 107.87. ESI-HRMS (m/z): [$\text{M} - \text{H}$] $^-$ calcd for $\text{C}_{22}\text{H}_{11}\text{F}_4\text{O}_2\text{S}$, 415.0416; observed, 415.0409.

(2-(4-Chlorophenyl)-6-hydroxybenzo[*b*]thiophen-3-yl)(4-(trifluoromethyl)phenyl)methanone (14c). This compound was isolated from the preparation of **14b** as a minor product, (130 mg, yield 3%). ^1H NMR (400 MHz, CD_3OD) δ 7.79 (d, J = 8.2 Hz, 2H), 7.65 (d, J = 8.8 Hz, 1H), 7.56 (d, J = 8.2 Hz, 2H), 7.31 (d, J = 2.2 Hz, 1H), 7.27 (d, J = 8.5 Hz, 2H), 7.19 (d, J = 8.5 Hz, 2H), 6.95 (dd, J = 8.8, 2.2 Hz, 1H). ^{13}C NMR (100 MHz, CD_3OD) δ 194.18, 157.53, 145.00, 142.23, 141.94, 135.98, 135.06 (q, $J_{\text{C-F}}$ = 32.5 Hz), 133.65, 133.35, 132.13, 131.91, 131.32, 129.79, 126.44 (q, $J_{\text{C-F}}$ = 3.8 Hz), 125.50, 125.10 (q, $J_{\text{C-F}}$ = 272 Hz), 116.76, 107.88. ESI-HRMS (m/z): [$\text{M} - \text{H}$] $^-$ calcd for $\text{C}_{22}\text{H}_{11}\text{ClF}_3\text{O}_2\text{S}$, 431.0120; observed, 431.0113.

2-(4-Fluorophenyl)-6-methoxy-3-(4-methoxyphenoxy)-benzo[*b*]thiophene 1-Oxide (17). NaH (380 mg, 9.5 mmol, 60% dispersion in mineral oil) was added in three portions to a flask charged with a solution of 4-methoxyphenol (0.85 g, 6.9 mmol) in 10 mL of anhydrous DMF under argon atmosphere at room temperature. After the mixture was stirred for 30 min, 3-bromo-2-(4-fluorophenyl)-6-methoxybenzo[*b*]thiophene 1-oxide³² (2.2 g, 6.3 mmol) was added in small portions. After the mixture was stirred for 2 h, ethyl acetate and water were added, and the organic layer was washed several times with water and brine, then dried over Na_2SO_4 . The residue was purified by flash chromatography (5–60% ethyl acetate in hexane) to yield 2.4 g (yield, 93%) of the title compound. ^1H NMR (400 MHz, CDCl_3) δ 7.78–7.72 (m, 2H), 7.50 (d, J = 2.3 Hz, 1H), 7.09–6.97 (m, 5H), 6.91 (dd, J = 8.5, 2.3 Hz, 1H), 6.83–6.76 (m, 2H), 3.88 (s, 3H), 3.76 (s, 3H). ^{13}C NMR (100 MHz, CDCl_3) δ 162.68 (d, $J_{\text{C-F}}$ = 249.6 Hz), 161.12, 156.29, 150.13, 149.01, 144.76, 130.26 (d, $J_{\text{C-F}}$ = 8.2 Hz), 130.19, 126.40, 125.94, 124.11, 118.24, 118.18, 116.04 (d, $J_{\text{C-F}}$ = 21.8 Hz), 115.03, 112.08, 56.10, 55.84.

2-(4-Fluorophenyl)-6-methoxy-3-(4-methoxyphenoxy)-benzo[*b*]thiophene (18). LiAlH_4 (372 mg, 9.8 mmol) was added in small portions to a solution of **17b** (2.6 g, 6.6 mmol) in 30 mL of anhydrous THF under argon atmosphere at 0 °C. After the mixture was stirred for 2 h, 0.4 mL of water was slowly added followed by 0.4 mL of 15% NaOH to quench the reaction. The precipitate was then filtered through Celite and washed with ethyl acetate. The filtrate was washed with water and brine three times. The organic layers were combined, dried over anhydrous Na_2SO_4 , and then purified by flash chromatography (1–30% ethyl acetate in hexane) to yield 1.8 g (yield, 71%) product. ^1H NMR (400 MHz, CDCl_3) δ 7.76–7.68 (m, 2H), 7.28–7.24 (m, 2H), 7.04 (t, J = 8.7 Hz, 2H), 6.94–6.85 (m, 3H), 6.83–6.75 (m, 2H), 3.87 (s, 3H), 3.75 (s, 3H). ^{13}C NMR (100 MHz, CDCl_3) δ 162.30 (d, $J_{\text{C-F}}$ = 248.0 Hz), 158.27, 155.06, 151.73, 140.81, 137.24, 129.34 (d, $J_{\text{C-F}}$ = 8.0 Hz), 128.38, 128.01, 125.52, 122.63, 116.52, 115.91 (d, $J_{\text{C-F}}$ = 21.6 Hz), 114.95, 114.68, 105.54, 55.80, 55.78.

2-(4-Fluorophenyl)-3-(4-hydroxyphenoxy)benzo[*b*]thiophen-6-ol (19). This compound was prepared by a procedure identical to the preparation of **11** (1.3 g, white solid, yield 78%). ^1H NMR (400 MHz, CD_3OD) δ 7.77–7.66 (m, 2H), 7.22–7.15 (m, 2H), 7.07 (t, J = 8.7 Hz, 2H), 6.83–6.72 (m, 3H), 6.71–6.64 (m, 2H). ^{13}C NMR (100 MHz, CD_3OD) δ 163.43 (d, $J_{\text{C-F}}$ = 246.6 Hz), 157.29,

153.68, 152.10, 142.36, 138.54, 130.31, 130.24 (d, $J_{\text{C-F}}$ = 8.0 Hz), 128.33, 125.19, 123.45, 117.35, 117.04, 116.52 (d, $J_{\text{C-F}}$ = 21.9 Hz), 115.67, 108.73. ESI-HRMS (m/z): [$\text{M} + \text{H}$] $^+$ calcd for $\text{C}_{20}\text{H}_{13}\text{FO}_3\text{S}$, 353.0648; observed, 353.0632.

(3-(4-Fluorophenyl)-6-methoxybenzo[*b*]thiophen-2-yl)(4-(methylsulfonyl)phenyl)methanone (20a). This compound was prepared by a procedure identical to the preparation of **13b** (180 mg, yield, 21%). ^1H NMR (400 MHz, CDCl_3) δ 7.71 (d, J = 8.3 Hz, 2H), 7.61 (d, J = 8.3 Hz, 2H), 7.55 (d, J = 9.0 Hz, 1H), 7.37 (d, J = 2.1 Hz, 1H), 7.17–7.13 (m, 2H), 7.04 (dd, J = 9.0, 2.1 Hz, 1H), 6.88 (t, J = 8.5 Hz, 2H), 3.94 (s, 3H), 2.97 (s, 3H). ^{13}C NMR (100 MHz, CDCl_3) δ 189.78, 162.61 (d, $J_{\text{C-F}}$ = 249.3 Hz), 160.49, 143.73, 142.96, 142.68, 142.37, 135.72, 133.52, 132.38 (d, $J_{\text{C-F}}$ = 8.2 Hz), 130.45 (d, $J_{\text{C-F}}$ = 3.5 Hz), 129.93, 126.95, 126.43, 116.70, 115.45 (d, $J_{\text{C-F}}$ = 21.6 Hz), 104.40, 55.92, 44.54.

(3-(4-Fluorophenyl)-6-methoxybenzo[*b*]thiophen-2-yl)(4-methoxyphenyl)methanone (20b). This compound was prepared by a procedure identical to the preparation of **13b** (488 mg, yield 52%). ^1H NMR (400 MHz, CDCl_3) δ 7.63–7.57 (m, 3H), 7.35 (d, J = 2.2 Hz, 1H), 7.29–7.21 (m, 2H), 7.02 (dd, J = 9.0, 2.3 Hz, 1H), 6.94 (t, J = 8.7 Hz, 2H), 6.68 (d, J = 8.8 Hz, 2H), 3.91 (s, 3H), 3.78 (s, 3H). ^{13}C NMR (100 MHz, CDCl_3) δ 189.74, 163.19, 162.48 (d, $J_{\text{C-F}}$ = 248.6 Hz), 159.49, 142.55, 139.65, 135.81, 133.37, 132.17, 131.98 (d, $J_{\text{C-F}}$ = 8.2 Hz), 130.86 (d, $J_{\text{C-F}}$ = 3.4 Hz), 130.51, 125.65, 115.96, 115.42 (d, $J_{\text{C-F}}$ = 21.6 Hz), 113.31, 104.41, 55.81, 55.53.

(4-(Dimethylamino)phenyl)(3-(4-fluorophenyl)-6-methoxybenzo[*b*]thiophen-2-yl)methanone (20c). This compound was prepared by a procedure identical to the preparation of **13b** (393 mg, yield 48%). ^1H NMR (400 MHz, CDCl_3) δ 7.66–7.58 (m, 3H), 7.36–7.30 (m, 3H), 7.09–6.92 (m, 3H), 6.44 (d, J = 9.0 Hz, 2H), 3.92 (s, 3H), 3.00 (s, 6H). ^{13}C NMR (100 MHz, CDCl_3) δ 188.84, 162.37 (d, $J_{\text{C-F}}$ = 247.1 Hz), 159.00, 153.43, 142.02, 137.96, 136.20, 133.30, 132.52, 131.85 (d, $J_{\text{C-F}}$ = 8.1 Hz), 131.16 (d, $J_{\text{C-F}}$ = 3.3 Hz), 125.18, 125.05, 115.58, 115.41 (d, $J_{\text{C-F}}$ = 21.5 Hz), 110.37, 104.49, 55.80, 40.09.

(3-(4-Fluorophenyl)-6-methoxybenzo[*b*]thiophen-2-yl)(*p*-tolyl)methanone (20d). This compound was prepared by a procedure identical to the preparation of **13b** (390 mg, yield 49%). ^1H NMR (400 MHz, CDCl_3) δ 7.58 (d, J = 9.0 Hz, 1H), 7.50 (d, J = 8.1 Hz, 2H), 7.35 (d, J = 2.2 Hz, 1H), 7.25–7.19 (m, 2H), 7.06–6.96 (m, 3H), 6.93 (t, J = 8.7 Hz, 2H), 3.93 (s, 3H), 2.30 (s, 3H). ^{13}C NMR (100 MHz, CDCl_3) δ 190.85, 162.51 (d, $J_{\text{C-F}}$ = 247.8 Hz), 159.62, 143.18, 142.74, 140.33, 135.82, 135.27, 133.46, 131.98 (d, $J_{\text{C-F}}$ = 8.2 Hz), 130.77 (d, $J_{\text{C-F}}$ = 3.4 Hz), 129.83, 128.64, 125.81, 116.02, 115.31 (d, $J_{\text{C-F}}$ = 21.6 Hz), 104.36, 55.79, 21.66.

(4-Fluorophenyl)(3-(4-fluorophenyl)-6-methoxybenzo[*b*]thiophen-2-yl)methanone (20e). This compound was prepared by a procedure identical to the preparation of **13b** (510 mg, yield 67%). ^1H NMR (400 MHz, CDCl_3) δ 7.64–7.54 (m, 3H), 7.36 (d, J = 2.2 Hz, 1H), 7.25–7.18 (m, 2H), 7.03 (dd, J = 9.0, 2.3 Hz, 1H), 6.94 (t, J = 8.6 Hz, 2H), 6.85 (t, J = 8.6 Hz, 2H), 3.92 (s, 3H). ^{13}C NMR (100 MHz, CDCl_3) δ 189.72, 165.14 (d, $J_{\text{C-F}}$ = 254.4 Hz), 162.61 (d, $J_{\text{C-F}}$ = 248.7 Hz), 159.87, 142.96, 140.74, 135.54, 134.24 (d, $J_{\text{C-F}}$ = 3.0 Hz), 133.43, 132.16 (d, $J_{\text{C-F}}$ = 9.5 Hz), 132.07 (d, $J_{\text{C-F}}$ = 8.5 Hz), 130.61 (d, $J_{\text{C-F}}$ = 3.4 Hz), 125.96, 116.24, 115.49 (d, $J_{\text{C-F}}$ = 21.7 Hz), 115.11 (d, $J_{\text{C-F}}$ = 22.0 Hz), 104.42, 55.84.

Cyclopropyl(3-(4-fluorophenyl)-6-methoxybenzo[*b*]thiophen-2-yl)methanone (20f). This compound was prepared by a procedure identical to the preparation of **13b** (450 mg, yield 69%). ^1H NMR (400 MHz, CDCl_3) δ 7.48–7.41 (m, 2H), 7.37 (d, J = 9.0 Hz, 1H), 7.31 (d, J = 2.3 Hz, 1H), 7.20 (dd, J = 12.0, 5.4 Hz, 2H), 6.97 (dd, J = 9.0, 2.3 Hz, 1H), 3.91 (s, 3H), 1.84–1.73 (m, 1H), 1.22–1.10 (m, 2H), 0.73 (dq, J = 7.1, 3.5 Hz, 2H). ^{13}C NMR (100 MHz, CDCl_3) δ 195.69, 163.02 (d, $J_{\text{C-F}}$ = 248.0 Hz), 159.99, 142.64, 140.19, 138.65, 134.86, 131.96 (d, $J_{\text{C-F}}$ = 8.1 Hz), 131.35, 126.28, 116.02, 115.84 (d, $J_{\text{C-F}}$ = 21.6 Hz), 104.34, 55.83, 20.65, 12.58.

Cyclohexyl(3-(4-fluorophenyl)-6-methoxybenzo[*b*]thiophen-2-yl)methanone (20g). This compound was prepared by a procedure identical to the preparation of **13b** (520 mg, yield 91%). ^1H NMR (400 MHz, CDCl_3) δ 7.37–7.31 (m, 2H), 7.28 (d, J = 2.2 Hz, 1H), 7.25 (d, J = 9.0 Hz, 1H), 7.21–7.17 (m, 2H), 6.93 (dd, J = 9.0, 2.3

Hz, 1H), 3.88 (s, 3H), 2.47 (ddd, $J = 11.7, 7.3, 2.8$ Hz, 1H), 1.77–1.60 (m, 4H), 1.54 (d, $J = 13.2$ Hz, 1H), 1.44–1.27 (m, 2H), 1.17–1.02 (m, 1H), 0.93–0.75 (m, 2H). ^{13}C NMR (100 MHz, CDCl_3) δ 199.25, 162.96 (d, $J_{\text{C-F}} = 248.2$ Hz), 159.99, 142.49, 139.95, 137.33, 135.15, 131.45, 131.43 (d, $J_{\text{C-F}} = 8.1$ Hz), 126.33, 115.72 (d, $J_{\text{C-F}} = 21.6$ Hz), 115.61, 104.25, 55.80, 48.44, 29.38, 25.81, 25.77.

(3-(4-Fluorophenyl)-6-methoxybenzo[*b*]thiophen-2-yl)(4-iodophenyl)methanone (20h). This compound was prepared by a procedure identical to the preparation of **13b** (982 mg, yield 26%). ^1H NMR (400 MHz, CDCl_3) δ 7.57–7.51 (m, 3H), 7.34 (d, $J = 2.1$ Hz, 1H), 7.26 (d, $J = 8.3$ Hz, 2H), 7.21–7.18 (m, 2H), 7.02 (dd, $J = 8.7, 2.1$ Hz, 1H), 6.94 (t, $J = 8.5$ Hz, 2H), 3.91 (s, 3H). ^{13}C NMR (100 MHz, CDCl_3) δ 190.27, 162.69 (d, $J_{\text{C-F}} = 248.9$ Hz), 159.94, 143.07, 141.17, 137.34, 137.18, 135.31, 133.43, 132.02 (d, $J_{\text{C-F}} = 8.2$ Hz), 130.84, 130.46 (d, $J_{\text{C-F}} = 3.4$ Hz), 126.06, 116.30, 115.50 (d, $J_{\text{C-F}} = 21.7$ Hz), 104.34, 99.73, 55.83.

(3-(4-Fluorophenyl)-6-hydroxybenzo[*b*]thiophen-2-yl)(4-methylsulfonylphenyl)methanone (21a). This compound was prepared by a procedure identical to the preparation of **11** (120 mg, light green solid, yield 85%). ^1H NMR (400 MHz, $\text{DMSO}-d_6$) δ 10.32 (s, 1H), 7.67 (d, $J = 8.4$ Hz, 2H), 7.60 (d, $J = 8.4$ Hz, 2H), 7.45–7.43 (m, 2H), 7.23 (dd, $J = 8.5, 5.6$ Hz, 2H), 7.02–6.98 (m, 3H), 3.14 (s, 3H). ^{13}C NMR (100 MHz, $\text{DMSO}-d_6$) δ 189.53, 161.80 (d, $J_{\text{C-F}} = 246.0$ Hz), 158.49, 142.71, 142.69, 142.43, 142.27, 134.29, 132.50 (d, $J_{\text{C-F}} = 8.5$ Hz), 132.15, 129.96, 129.35, 126.53, 126.26, 116.59, 114.94 (d, $J_{\text{C-F}} = 21.6$ Hz), 107.22, 43.38. ESI-HRMS (m/z): $[\text{M} - \text{H}]^-$ calcd for $\text{C}_{22}\text{H}_{14}\text{FO}_4\text{S}_2$, 425.0318; observed, 425.0326.

(3-(4-Fluorophenyl)-6-hydroxybenzo[*b*]thiophen-2-yl)(4-hydroxyphenyl)methanone (21b). This compound was prepared by a procedure identical to the preparation of **11** (284 mg, white solid, yield 53%). ^1H NMR (400 MHz, CD_3OD) δ 7.51–7.44 (m, 3H), 7.29 (d, $J = 2.0$ Hz, 1H), 7.25–7.22 (m, 2H), 7.02–6.88 (m, 3H), 6.57 (d, $J = 8.7$ Hz, 2H). ^{13}C NMR (100 MHz, CD_3OD) δ 192.04, 163.79 (d, $J_{\text{C-F}} = 243.1$ Hz), 163.31, 158.86, 143.82, 141.34, 135.99, 133.64, 133.48, 133.28 (d, $J_{\text{C-F}} = 8.3$ Hz), 132.34 (d, $J_{\text{C-F}} = 3.4$ Hz), 130.33, 126.72, 116.95, 116.13 (d, $J_{\text{C-F}} = 21.9$ Hz), 115.75, 107.96. ESI-HRMS (m/z): $[\text{M} + \text{H}]^+$ calcd for $\text{C}_{21}\text{H}_{14}\text{FO}_3\text{S}$, 365.0648; observed, 365.0638.

(4-(Dimethylamino)phenyl)(3-(4-fluorophenyl)-6-hydroxybenzo[*b*]thiophen-2-yl)methanone (21c). This compound was prepared by a procedure identical to the preparation of **11** (205 mg, white solid, yield 54%). ^1H NMR (400 MHz, CD_3OD) δ 7.54 (dd, $J = 9.0, 2.9$ Hz, 3H), 7.37–7.27 (m, 3H), 7.01 (t, $J = 8.8$ Hz, 2H), 6.96 (dd, $J = 8.8, 2.2$ Hz, 1H), 6.51 (d, $J = 9.1$ Hz, 2H), 3.00 (s, 6H). ^{13}C NMR (100 MHz, CD_3OD) δ 191.43, 163.72 (d, $J_{\text{C-F}} = 246.2$ Hz), 158.47, 155.26, 143.39, 139.88, 136.14, 133.63, 133.52, 133.15 (d, $J_{\text{C-F}} = 8.3$ Hz), 132.61, 126.30, 125.62, 116.76, 116.20 (d, $J_{\text{C-F}} = 21.9$ Hz), 111.47, 107.99, 40.04. ESI-HRMS (m/z): $[\text{M} + \text{H}]^+$ calcd for $\text{C}_{23}\text{H}_{19}\text{FNO}_2\text{S}$, 392.1121; observed, 392.1113.

(3-(4-Fluorophenyl)-6-hydroxybenzo[*b*]thiophen-2-yl)(*p*-tolyl)methanone (21d). This compound was prepared by a procedure identical to the preparation of **11** (190 mg, white solid, yield 52%). ^1H NMR (400 MHz, $\text{DMSO}-d_6$) δ 10.18 (s, 1H), 7.52–7.38 (m, 4H), 7.32–7.27 (m, 2H), 7.11–7.02 (m, 4H), 6.99 (dd, $J = 8.9, 2.1$ Hz, 1H), 2.26 (s, 3H). ^{13}C NMR (100 MHz, $\text{DMSO}-d_6$) δ 190.37, 162.18 (d, $J_{\text{C-F}} = 245.3$ Hz), 158.18, 142.94, 142.32, 140.76, 135.37, 134.48, 132.57 (d, $J_{\text{C-F}} = 8.3$ Hz), 132.27, 130.98 (d, $J_{\text{C-F}} = 3.1$ Hz), 129.70, 128.90, 126.24, 116.74, 115.51 (d, $J_{\text{C-F}} = 21.6$ Hz), 107.61, 21.50. ESI-HRMS (m/z): $[\text{M} + \text{H}]^+$ calcd for $\text{C}_{22}\text{H}_{16}\text{FO}_2\text{S}$, 363.0855; observed, 363.0860.

(4-Fluorophenyl)(3-(4-fluorophenyl)-6-hydroxybenzo[*b*]thiophen-2-yl)methanone (21e). This compound was prepared by a procedure identical to the preparation of **11** (211 mg, green solid, yield 61%). ^1H NMR (400 MHz, acetone- d_6) δ 7.68–7.59 (m, 2H), 7.56 (d, $J = 8.9$ Hz, 1H), 7.47 (d, $J = 2.2$ Hz, 1H), 7.39–7.29 (m, 2H), 7.09–7.02 (m, 3H), 7.01–6.94 (m, 2H). ^{13}C NMR (100 MHz, CDCl_3) δ 189.93, 165.28 (d, $J_{\text{C-F}} = 251.6$ Hz), 163.04 (d, $J_{\text{C-F}} = 247.5$ Hz), 158.70, 143.53, 141.59, 135.85, 135.49 (d, $J_{\text{C-F}} = 3.0$ Hz), 133.55, 133.30 (d, $J_{\text{C-F}} = 8.3$ Hz), 132.85 (d, $J_{\text{C-F}} = 9.3$ Hz), 131.69 (d, $J_{\text{C-F}} = 3.3$ Hz), 126.95, 116.95, 115.92 (d, $J_{\text{C-F}} = 21.8$ Hz), 115.60 (d, $J_{\text{C-F}} = 22.2$ Hz), 108.02. ESI-HRMS (m/z): $[\text{M} - \text{H}]^-$ calcd for $\text{C}_{21}\text{H}_{11}\text{F}_2\text{O}_2\text{S}$, 365.0448; observed, 365.0444.

Cyclopropyl(3-(4-fluorophenyl)-6-hydroxybenzo[*b*]thiophen-2-yl)methanone (21f). NaO t Bu (280 mg, 3.6 mmol) was added to an oven-dried round-bottom flask charged with 2-(dimethylamino)ethanethiol hydrochloride (305 mg, 1.8 mmol) in 3 mL of DMF in an ice bath. After 15 min, the mixture was allowed to equilibrate to room temperature, and one portion of **20f** (400 mg, 1.2 mmol) was added, and the mixture was heated to reflux. The reaction was monitored by TLC and quenched by ice–water. Ethyl acetate and water were added, and the organic layer was washed several times with water and brine, then dried over Na_2SO_4 . The residue was purified by flash chromatography (5–40% ethyl acetate in hexane) to yield 94 mg (yield, 25%) of the title compound. ^1H NMR (400 MHz, acetone- d_6) δ 7.62–7.51 (m, 2H), 7.39 (d, $J = 2.1$ Hz, 1H), 7.38–7.31 (m, 3H), 7.00 (dd, $J = 8.9, 2.2$ Hz, 1H), 1.80 (tt, $J = 7.8, 4.6$ Hz, 1H), 1.05–0.97 (m, 2H), 0.75–0.69 (m, 2H). ^{13}C NMR (100 MHz, acetone- d_6) δ 195.38, 163.89 (d, $J_{\text{C-F}} = 246.2$ Hz), 158.91, 143.34, 141.12, 138.83, 135.01, 133.14 (d, $J_{\text{C-F}} = 8.3$ Hz), 132.43 (d, $J_{\text{C-F}} = 3.4$ Hz), 127.34, 116.86, 116.57 (d, $J_{\text{C-F}} = 21.7$ Hz), 108.01, 20.97, 12.32. ESI-HRMS (m/z): $[\text{M} + \text{H}]^+$ calcd for $\text{C}_{18}\text{H}_{14}\text{FO}_2\text{S}$, 313.0699; observed, 313.0696.

Cyclohexyl(3-(4-fluorophenyl)-6-hydroxybenzo[*b*]thiophen-2-yl)methanone (21g). **20g** (6.56 g, 18 mmol) was dissolved in 50 mL of anhydrous dichloromethane and cooled to -78°C in a dry ice–acetone bath. $\text{BF}_3 \cdot \text{SMe}_2$ (23.4 g, 180 mmol) was added dropwise to this solution. The reaction mixture was stirred until starting material was consumed as monitored by TLC and then quenched by saturated NaHCO_3 /ice–water. The reaction mixture was extracted with ethyl acetate and washed with brine. The organic extracts were combined, dried over anhydrous Na_2SO_4 , concentrated in vacuo, and then purified by flash chromatography (5–60% ethyl acetate in hexane) to give 4.8 g of white powder (yield, 76%). ^1H NMR (400 MHz, CD_3OD) δ 7.46–7.38 (m, 2H), 7.31 (t, $J = 8.8$ Hz, 2H), 7.23 (d, $J = 2.2$ Hz, 1H), 7.19 (d, $J = 8.9$ Hz, 1H), 6.88 (dd, $J = 8.9, 2.2$ Hz, 1H), 2.51 (tt, $J = 11.5, 2.9$ Hz, 1H), 1.68–1.64 (m, 4H), 1.57–1.54 (m, 1H), 1.37–1.23 (m, 2H), 1.19–1.05 (m, 1H), 0.92–0.77 (m, 2H). ^{13}C NMR (100 MHz, CD_3OD) δ 201.15, 164.43 (d, $J_{\text{C-F}} = 246.9$ Hz), 159.63, 144.07, 142.15, 137.60, 135.51, 133.00, 132.74 (d, $J_{\text{C-F}} = 8.2$ Hz), 127.58, 117.02, 116.64 (d, $J_{\text{C-F}} = 21.9$ Hz), 107.78, 49.50, 30.40, 26.79, 26.76. ESI-HRMS (m/z): $[\text{M} + \text{H}]^+$ calcd for $\text{C}_{21}\text{H}_{20}\text{FO}_2\text{S}$, 355.1168; observed, 355.1150.

(4-Ethynylphenyl)(3-(4-fluorophenyl)-6-methoxybenzo[*b*]thiophen-2-yl)methanone (22). To a mixture of **20h** (244 mg, 0.5 mmol) and ethynyltrimethylsilane (108 mg, 0.55 mmol) in dry trimethylamine (5 mL) were added $\text{Pd}(\text{PPh}_3)_2\text{Cl}_2$ (5% mol) and CuI (5% mol) under argon atmosphere. The mixture was heated at 70°C . After cooling the mixture to room temperature, ethyl acetate was added and the suspension was filtered through a pad of silica gel. The filtrate was collected, and the crude product was treated with 1 M TBAF (1.5 equiv) in THF. After 30 min, the reaction was quenched by pouring into ice–water and extracted with ethyl acetate. The organic phase was washed with brine and dried over Na_2SO_4 . The mixture was purified by flash chromatography (1–30% ethyl acetate in hexane) to give the title product (96 mg, yield 50%). ^1H NMR (400 MHz, CDCl_3) δ 7.57 (d, $J = 9.0$ Hz, 1H), 7.51 (d, $J = 8.4$ Hz, 2H), 7.35 (d, $J = 2.2$ Hz, 1H), 7.28 (d, $J = 8.3$ Hz, 2H), 7.24–7.16 (m, 2H), 7.03 (dd, $J = 9.0, 2.3$ Hz, 1H), 6.93 (t, $J = 8.6$ Hz, 2H), 3.92 (s, 3H), 3.18 (s, 1H). ^{13}C NMR (100 MHz, CDCl_3) δ 190.35, 162.67 (d, $J_{\text{C-F}} = 248.8$ Hz), 159.93, 143.10, 141.10, 137.90, 135.53, 133.46, 132.06 (d, $J_{\text{C-F}} = 8.2$ Hz), 131.61, 130.51 (d, $J_{\text{C-F}} = 3.5$ Hz), 129.41, 126.06, 125.94, 116.29, 115.49 (d, $J_{\text{C-F}} = 21.7$ Hz), 104.37, 82.92, 80.08, 55.84.

(4-Ethynylphenyl)(3-(4-fluorophenyl)-6-hydroxybenzo[*b*]thiophen-2-yl)methanone (23). This compound was prepared by a procedure identical to the preparation of **21g** (704 mg, yellow solid, yield 56%). ^1H NMR (400 MHz, acetone- d_6) δ 7.57–7.52 (m, 3H), 7.47 (d, $J = 2.2$ Hz, 1H), 7.37–7.28 (m, 4H), 7.08–7.00 (m, 3H), 3.81 (s, 1H). ^{13}C NMR (100 MHz, acetone- d_6) δ 190.56, 163.39 (d, $J_{\text{C-F}} = 246.4$ Hz), 158.76, 143.71, 141.93, 139.09, 135.87, 133.64, 133.31 (d, $J_{\text{C-F}} = 8.3$ Hz), 132.15, 131.67 (d, $J_{\text{C-F}} = 3.4$ Hz), 130.12, 127.06, 126.43, 116.99, 115.93 (d, $J_{\text{C-F}} = 21.8$ Hz), 108.03, 83.44, 81.75. ESI-HRMS (m/z): $[\text{M} + \text{H}]^+$ calcd for $\text{C}_{23}\text{H}_{14}\text{FO}_3\text{S}$, 373.0699; observed, 373.0686.

2-Bromo-3-(4-fluorophenyl)-6-methoxybenzo[*b*]thiophene (24). *N*-Bromoacetamide (1.46 g, 10.5 mmol) was added in small

portions to a solution of **10** (2.58 g, 10 mmol) in 300 mL of CH_2Cl_2 and 20 mL of ethanol at room temperature. After the mixture was stirred for 1 h, the solvent was removed in vacuo. The residue was titrated with pure ethanol and filtered to give 3.0 g (yield, 89%) of white powder. ^1H NMR (400 MHz, CDCl_3) δ 7.47–7.41 (m, 2H), 7.39 (d, J = 8.9 Hz, 1H), 7.24 (d, J = 2.3 Hz, 1H), 7.23–7.17 (m, 2H), 6.94 (dd, J = 8.9, 2.4 Hz, 1H), 3.87 (s, 3H). ^{13}C NMR (100 MHz, CDCl_3) δ 162.63 (d, $J_{\text{C-F}}$ = 247.5 Hz), 157.89, 157.88, 141.13, 135.81, 132.81, 131.79 (d, $J_{\text{C-F}}$ = 8.1 Hz), 130.10 (d, $J_{\text{C-F}}$ = 3.3 Hz), 123.51, 115.78 (d, $J_{\text{C-F}}$ = 21.6 Hz), 114.72, 104.66, 55.80.

(3-(4-Fluorophenyl)-6-methoxybenzo[b]thiophen-2-yl)(4-(trifluoromethyl)phenyl)methanone (25a). To an oven-dried flask charged with **24** (7.4 g, 21.8 mmol) in 40 mL of THF in a dry ice–acetone bath, $n\text{-BuLi}$ (1.6 M, 15 mL) was added dropwise under argon atmosphere. After stirring for 30 min, a solution of 4-(trifluoromethyl)benzoyl chloride (5 g, 24 mmol) in 10 mL of THF was added dropwise. The reaction was allowed to warm to room temperature and was monitored by TLC. Upon the consumption of the starting material, the reaction was poured into ice–water. The mixture was extracted with ethyl acetate, washed with brine, and then dried over anhydrous Na_2SO_4 . The crude product was purified by flash chromatography (1–30% ethyl acetate in hexane) to give the title product (5.3 g, yield 57%). ^1H NMR (400 MHz, CDCl_3) δ 7.59–7.55 (m, 3H), 7.42–7.36 (m, 3H), 7.18–7.13 (m, 2H), 7.03 (dd, J = 9.0, 2.1 Hz, 1H), 6.88 (t, J = 8.5 Hz, 2H), 3.93 (s, 3H). ^{13}C NMR (100 MHz, CDCl_3) δ 190.14, 162.71 (d, $J_{\text{C-F}}$ = 249.5 Hz), 160.27, 143.46, 142.08, 141.28, 135.58, 133.59, 133.20 (q, $J_{\text{C-F}}$ = 32.7 Hz), 132.13 (d, $J_{\text{C-F}}$ = 8.2 Hz), 130.29 (d, $J_{\text{C-F}}$ = 3.4 Hz), 129.51, 126.35, 124.84 (q, $J_{\text{C-F}}$ = 3.7 Hz), 123.63 (q, $J_{\text{C-F}}$ = 272.9 Hz), 116.50, 115.46 (d, $J_{\text{C-F}}$ = 21.8 Hz), 104.37, 55.87.

4-(3-(4-Fluorophenyl)-6-methoxybenzo[b]thiophene-2-carbonyl)benzonitrile (25b). This compound was prepared by a procedure identical to the preparation of **25a** (420 mg, yield 54%). ^1H NMR (400 MHz, CDCl_3) δ 7.56 (t, J = 8.1 Hz, 3H), 7.44 (d, J = 8.4 Hz, 2H), 7.36 (d, J = 2.3 Hz, 1H), 7.20–7.13 (m, 2H), 7.04 (dd, J = 9.0, 2.3 Hz, 1H), 6.95–6.88 (m, 2H), 3.93 (s, 3H). ^{13}C NMR (100 MHz, CDCl_3) δ 189.50, 162.61 (d, $J_{\text{C-F}}$ = 250.0 Hz), 160.22, 143.41, 141.99, 141.66, 135.04, 133.30, 132.03 (d, $J_{\text{C-F}}$ = 8.2 Hz), 131.52, 130.09 (d, $J_{\text{C-F}}$ = 3.5 Hz), 129.51, 126.21, 117.87, 116.48, 115.46 (d, $J_{\text{C-F}}$ = 21.7 Hz), 114.91, 104.23, 55.75.

(3-(4-Fluorophenyl)-6-hydroxybenzo[b]thiophen-2-yl)(4-(trifluoromethyl)phenyl)methanone (26a). This compound was prepared by a procedure identical to the preparation of **11** (3.8 g, light green powder, yield 82%). ^1H NMR (400 MHz, acetone- d_6) δ 7.65 (d, J = 8.0 Hz, 2H), 7.53 (t, J = 9.1 Hz, 3H), 7.48 (d, J = 2.2 Hz, 1H), 7.33–7.22 (m, 2H), 7.06 (dd, J = 8.9, 2.2 Hz, 1H), 6.97 (t, J = 8.8 Hz, 2H). ^{13}C NMR (100 MHz, acetone- d_6) δ 190.61, 163.52 (d, $J_{\text{C-F}}$ = 246.9 Hz), 159.21, 144.17, 143.13, 142.97, 136.13, 133.92, 133.55 (d, $J_{\text{C-F}}$ = 8.4 Hz), 132.93 (q, $J_{\text{C-F}}$ = 32.2 Hz), 131.52 (d, $J_{\text{C-F}}$ = 3.4 Hz), 130.47, 127.51, 125.65 (q, $J_{\text{C-F}}$ = 3.9 Hz), 124.93 (q, $J_{\text{C-F}}$ = 271.1 Hz), 117.22, 115.99 (d, $J_{\text{C-F}}$ = 21.9 Hz), 108.13. ESI-HRMS (m/z): $[\text{M} + \text{H}]^+$ calcd for $\text{C}_{22}\text{H}_{13}\text{F}_4\text{O}_2\text{S}$, 417.0572; observed, 417.0563.

4-(3-(4-Fluorophenyl)-6-hydroxybenzo[b]thiophene-2-carbonyl)benzonitrile (26b). This compound was prepared by a procedure identical to the preparation of **11** (95 mg, yield 23%). ^1H NMR (400 MHz, CDCl_3) δ 7.60–7.54 (m, 3H), 7.45 (d, J = 8.5 Hz, 2H), 7.34 (d, J = 2.2 Hz, 1H), 7.21–7.13 (m, 2H), 6.98 (dd, J = 8.9, 2.3 Hz, 1H), 6.96–6.86 (m, 2H). ^{13}C NMR (100 MHz, CDCl_3) δ 189.77, 162.81 (d, $J_{\text{C-F}}$ = 250.1 Hz), 156.43, 143.41, 142.17, 141.78, 135.24, 133.72, 132.17 (d, $J_{\text{C-F}}$ = 8.2 Hz), 131.72, 130.21, 129.68, 126.82, 117.99, 116.22, 115.65 (d, $J_{\text{C-F}}$ = 21.7 Hz), 115.14, 107.73. ESI-HRMS (m/z): $[\text{M} - \text{H}]^-$ calcd for $\text{C}_{22}\text{H}_{11}\text{FNO}_2\text{S}$, 372.0495; observed, 372.0487.

2-Bromo-3-(4-fluorophenyl)-6-methoxybenzo[b]thiophene 1-Oxide (27). Trifluoroacetic acid (13 mL) was added dropwise to a solution of **24** (2.4 g, 7 mmol) in 13 mL of anhydrous CH_2Cl_2 in an ice bath. The mixture was stirred for 5 min, H_2O_2 (1.0 mL, 7 mmol, 30% aqueous solution) was added dropwise, and the resulting mixture was allowed to warm to room temperature and stirred for 2 h. Upon the consumption of starting material, sodium bisulfite (0.3 g) was added to the solution followed by 5 mL of water. The mixture was stirred

vigorously for 30 min and then concentrated in vacuo. The residue was partitioned between CH_2Cl_2 and saturated aqueous NaHCO_3 solution. The layers were separated, and the organic layer was washed with water, saturated NaHCO_3 , and water and then dried over anhydrous Na_2SO_4 . The residue was titrated with diethyl ether and filtered to give 2.1 g (yield, 84%) of pale yellow powder. ^1H NMR (400 MHz, CDCl_3) δ 7.52–7.45 (m, 3H), 7.25–7.20 (m, 2H), 7.16 (d, J = 8.5 Hz, 1H), 6.97 (dd, J = 8.5, 2.4 Hz, 1H), 3.89 (s, 3H). ^{13}C NMR (100 MHz, CDCl_3) δ 163.45 (d, $J_{\text{C-F}}$ = 250.6 Hz), 160.84, 146.91, 144.07, 130.87 (d, $J_{\text{C-F}}$ = 8.7 Hz), 130.86, 127.36 (d, $J_{\text{C-F}}$ = 3.5 Hz), 125.09, 124.75, 118.07, 116.35 (d, $J_{\text{C-F}}$ = 21.9 Hz), 112.84, 56.13.

3-(4-Fluorophenyl)-6-methoxy-2-(4-methoxyphenoxy)-benzo[b]thiophene 1-Oxide (28a). This compound was prepared by a procedure identical to the preparation of **17** (2.47 g, yellow solid, yield 89%). ^1H NMR (400 MHz, CDCl_3) δ 7.51–7.48 (m, 2H), 7.41 (d, J = 2.3 Hz, 1H), 7.26 (d, J = 8.5, 1H), 7.17–7.05 (m, 4H), 6.99 (dd, J = 8.5, 2.3 Hz, 1H), 6.81 (d, J = 9.0 Hz, 2H), 3.88 (s, 3H), 3.77 (s, 3H). ^{13}C NMR (100 MHz, CDCl_3) δ 163.14 (d, $J_{\text{C-F}}$ = 249.7 Hz), 160.47, 157.89, 156.42, 150.83, 142.13, 130.80 (d, $J_{\text{C-F}}$ = 8.3 Hz), 129.34, 128.00, 126.13 (d, $J_{\text{C-F}}$ = 3.4 Hz), 124.35, 118.76, 118.01, 116.14 (d, $J_{\text{C-F}}$ = 21.7 Hz), 114.92, 112.92, 56.06, 55.80.

2-(4-Chlorophenoxy)-3-(4-fluorophenyl)-6-methoxybenzo[b]thiophene 1-Oxide (28b). To an oven-dried flask charged with 4-chlorophenol in 10 mL of DMF, Cs_2CO_3 (1.3 g, 4 mmol) was added in a portion. After 15 min, **27** (702 mg, 2 mmol) was added slowly. The reaction was heated to 80 °C until the consumption of starting material. The mixture was quenched by ice–water and extracted with ethyl acetate and washed with water and brine. The crude material was then purified by flash chromatography (5–40% ethyl acetate in hexane) to give 403 mg (yield, 50%) of the title compound. ^1H NMR (400 MHz, CDCl_3) δ 7.50–7.44 (m, 3H), 7.31–7.24 (m, 3H), 7.20–7.08 (m, 4H), 7.03 (dd, J = 8.5, 2.5 Hz, 1H), 3.91 (s, 3H). ^{13}C NMR (100 MHz, CDCl_3) δ 163.29 (d, $J_{\text{C-F}}$ = 250.32 Hz), 160.82, 156.39, 155.68, 142.42, 130.72 (d, $J_{\text{C-F}}$ = 8.36 Hz), 130.10, 129.90, 129.35, 128.75, 125.76 (d, $J_{\text{C-F}}$ = 4 Hz), 124.73, 118.48, 118.18, 116.28 (d, $J_{\text{C-F}}$ = 21.8 Hz), 112.89, 56.10.

2-(4-Fluorophenoxy)-3-(4-fluorophenyl)-6-methoxybenzo[b]thiophene 1-Oxide (28c). This compound was prepared by a procedure identical to the preparation of **28b** (240 mg, yield 63%). ^1H NMR (400 MHz, CDCl_3) δ 7.49–7.44 (m, 2H), 7.43 (d, J = 2.4 Hz, 1H), 7.27 (d, J = 8.6 Hz, 1H), 7.18–7.07 (m, 4H), 7.04–6.91 (m, 3H), 3.88 (s, 3H). ^{13}C NMR (100 MHz, CDCl_3) δ 163.20 (d, $J_{\text{C-F}}$ = 250.1 Hz), 160.67, 159.28 (d, $J_{\text{C-F}}$ = 242.7 Hz), 157.04, 152.95 (d, $J_{\text{C-F}}$ = 2.5 Hz), 142.22, 130.73 (d, $J_{\text{C-F}}$ = 8.3 Hz), 129.24, 128.92, 125.84 (d, $J_{\text{C-F}}$ = 3.5 Hz), 124.59, 118.72 (d, $J_{\text{C-F}}$ = 8.4 Hz), 118.10, 116.44 (d, $J_{\text{C-F}}$ = 24.2 Hz), 116.21 (d, $J_{\text{C-F}}$ = 22.3 Hz), 112.88, 56.07.

3-(4-Fluorophenyl)-6-methoxy-2-(4-methoxyphenoxy)-benzo[b]thiophene (29a). This compound was prepared by a procedure identical to the preparation of **18** (1.2 g, white solid, yield 67%). ^1H NMR (400 MHz, CDCl_3) δ 7.56–7.48 (m, 3H), 7.20 (d, J = 2.4 Hz, 1H), 7.15–7.10 (m, 2H), 7.05–7.01 (m, 2H), 6.97 (dd, J = 8.8, 2.4 Hz, 1H), 6.85–6.77 (m, 2H), 3.86 (s, 3H), 3.78 (s, 3H). ^{13}C NMR (100 MHz, CDCl_3) δ 162.19 (d, $J_{\text{C-F}}$ = 246.5 Hz), 157.42, 156.22, 153.10, 152.53, 134.57, 131.21 (d, $J_{\text{C-F}}$ = 8.0 Hz), 131.08, 129.05, 123.11, 120.80, 118.61, 115.71 (d, $J_{\text{C-F}}$ = 21.4 Hz), 114.80, 114.22, 106.03, 55.86, 55.82.

2-(4-Chlorophenoxy)-3-(4-fluorophenyl)-6-methoxybenzo[b]thiophene (29b). This compound was prepared by a procedure identical to the preparation of **18** (206 mg, yield 53%). ^1H NMR (400 MHz, CDCl_3) δ 7.54 (d, J = 8.8 Hz, 1H), 7.49–7.43 (m, 2H), 7.26–7.21 (m, 3H), 7.11 (t, J = 8.8 Hz, 2H), 7.02–6.96 (m, 3H), 3.88 (s, 3H). ^{13}C NMR (100 MHz, CDCl_3) δ 162.32 (d, $J_{\text{C-F}}$ = 247.2 Hz), 157.80, 157.28, 150.75, 135.01, 131.12 (d, $J_{\text{C-F}}$ = 8.1 Hz), 130.78, 129.75, 128.77, 128.62 (d, $J_{\text{C-F}}$ = 3.4 Hz), 123.50, 122.84, 118.08, 115.83 (d, $J_{\text{C-F}}$ = 21.5 Hz), 114.52, 105.98, 55.87.

2-(4-Fluorophenoxy)-3-(4-fluorophenyl)-6-methoxybenzo[b]thiophene (29c). This compound was prepared by a procedure identical to the preparation of **18** (340 mg, yield 83%). ^1H NMR (400 MHz, CDCl_3) δ 7.53 (d, J = 8.8 Hz, 1H), 7.51–7.42 (m, 2H), 7.23 (d, J = 2.4 Hz, 1H), 7.12 (t, J = 8.7 Hz, 2H), 7.06–6.92 (m, 5H), 3.87 (s, 3H).

^{13}C NMR (100 MHz, CDCl_3) δ 162.10 (d, $J_{\text{C-F}} = 247.0$ Hz), 158.87 (d, $J_{\text{C-F}} = 242.2$ Hz), 157.51, 154.46 (d, $J_{\text{C-F}} = 2.5$ Hz), 151.58, 134.63, 130.99 (d, $J_{\text{C-F}} = 8.0$ Hz), 130.71, 128.58 (d, $J_{\text{C-F}} = 3.3$ Hz), 123.19, 121.90, 118.19 (d, $J_{\text{C-F}} = 8.3$ Hz), 116.12 (d, $J_{\text{C-F}} = 23.6$ Hz), 115.60 (d, $J_{\text{C-F}} = 21.5$ Hz), 114.25, 105.83, 55.68.

2-(3,4-Difluorophenoxy)-3-(4-fluorophenyl)-6-methoxybenzo[b]thiophene (29d). This compound was prepared by a procedure identical to the preparation of **18** (330 mg, yield 73%). ^1H NMR (400 MHz, CDCl_3) δ 7.54 (d, $J = 8.8$ Hz, 1H), 7.47–7.44 (m, 2H), 7.24 (d, $J = 2.1$ Hz, 1H), 7.15–7.03 (m, 3H), 7.00 (dd, $J = 8.9$, 2.1 Hz, 1H), 6.92–6.83 (m, 1H), 6.77 (d, $J = 9.1$ Hz, 1H), 3.88 (s, 3H).

3-(4-Fluorophenyl)-2-(4-hydroxyphenoxy)benzo[b]thiophen-6-ol (30a). This compound was prepared by a procedure identical to the preparation of **11** (1.1 g, white powder, yield 75%). ^1H NMR (400 MHz, acetone- d_6) δ 7.62–7.57 (m, 2H), 7.46 (d, $J = 8.7$ Hz, 1H), 7.30–7.19 (m, 3H), 7.05–6.97 (m, 2H), 6.95 (dd, $J = 8.7$, 2.3 Hz, 1H), 6.86–6.78 (m, 2H). ^{13}C NMR (100 MHz, CDCl_3) δ 162.57 (d, $J_{\text{C-F}} = 245.0$ Hz), 155.67, 154.69, 153.54, 152.12, 135.01, 131.97 (d, $J_{\text{C-F}} = 8.1$ Hz), 130.64, 130.04 (d, $J_{\text{C-F}} = 3.2$ Hz), 123.50, 120.60, 119.42, 116.76, 116.03 (d, $J_{\text{C-F}} = 21.5$ Hz), 115.35, 108.84. ESI-HRMS (m/z): $[\text{M} - \text{H}]^-$ calcd for $\text{C}_{20}\text{H}_{12}\text{FO}_3\text{S}$, 351.0491; observed, 351.0490.

2-(4-Chlorophenoxy)-3-(4-fluorophenyl)benzo[b]thiophen-6-ol (30b). This compound was prepared by a procedure identical to the preparation of **11** (140 mg, white powder, yield 73%). ^1H NMR (400 MHz, CDCl_3) δ 7.51 (d, $J = 8.7$ Hz, 1H), 7.49–7.42 (m, 2H), 7.26–7.21 (m, 2H), 7.20 (d, $J = 2.3$ Hz, 1H), 7.11 (t, $J = 8.7$ Hz, 2H), 7.03–6.97 (m, 2H), 6.91 (dd, $J = 8.7$, 2.4 Hz, 1H). ^{13}C NMR (100 MHz, CDCl_3) δ 162.34 (d, $J_{\text{C-F}} = 247.3$ Hz), 157.20, 153.43, 150.89, 135.05, 131.13 (d, $J_{\text{C-F}} = 8.1$ Hz), 129.76, 128.85, 128.55 (d, $J_{\text{C-F}} = 3$ Hz), 123.68, 122.71, 118.14, 115.84 (d, $J_{\text{C-F}} = 21.5$ Hz), 114.61, 108.53. ESI-HRMS (m/z): $[\text{M} + \text{H}]^+$ calcd for $\text{C}_{20}\text{H}_{11}\text{ClFO}_2\text{S}$, 369.0152; observed, 369.0144.

2-(4-Fluorophenoxy)-3-(4-fluorophenyl)benzo[b]thiophen-6-ol (30c). This compound was prepared by a procedure identical to the preparation of **11** (248 mg, white solid, yield 79%). ^1H NMR (400 MHz, CDCl_3) δ 7.56–7.41 (m, 3H), 7.18 (d, $J = 2.3$ Hz, 1H), 7.12 (t, $J = 8.7$ Hz, 2H), 7.06–6.92 (m, 4H), 6.90 (dd, $J = 8.7$, 2.4 Hz, 1H), 4.83 (s, 1H). ^{13}C NMR (100 MHz, CDCl_3) δ 162.12 (d, $J_{\text{C-F}} = 247.1$ Hz), 158.91 (d, $J_{\text{C-F}} = 242.4$ Hz), 154.39, 153.15, 151.73, 134.68, 131.00, 130.99 (d, $J_{\text{C-F}} = 8.1$ Hz), 128.53 (d, $J_{\text{C-F}} = 3.4$ Hz), 123.36, 121.76, 118.27 (d, $J_{\text{C-F}} = 8.3$ Hz), 116.14 (d, $J_{\text{C-F}} = 23.6$ Hz), 115.61 (d, $J_{\text{C-F}} = 21.5$ Hz), 114.37, 108.33. ESI-HRMS (m/z): $[\text{M} - \text{H}]^-$ calcd for $\text{C}_{20}\text{H}_{11}\text{F}_2\text{O}_2\text{S}$, 353.0448; observed, 353.0451.

2-(3,4-Difluorophenoxy)-3-(4-fluorophenyl)benzo[b]thiophen-6-ol (30d). This compound was prepared by a procedure identical to the preparation of **11** (83 mg, yield 61%). ^1H NMR (400 MHz, CDCl_3) δ 7.50 (d, $J = 8.7$ Hz, 1H), 7.45 (dd, $J = 8.2$, 5.9 Hz, 2H), 7.21 (d, $J = 2.1$ Hz, 1H), 7.17–7.00 (m, 3H), 6.97–6.83 (m, 2H), 6.79–6.75 (m, 1H), 4.85 (s, 1H). ^{13}C NMR (100 MHz, CDCl_3) δ 162.4 (d, $J_{\text{C-F}} = 247.4$ Hz), 154.46 (dd, $J_{\text{C-F}} = 8.0$, 2.4 Hz), 153.59, 150.60 (dd, $J_{\text{C-F}} = 249.9$, 14.2 Hz), 150.59 (d, $J_{\text{C-F}} = 249.7$ Hz), 146.91 (dd, $J_{\text{C-F}} = 244.0$, 13.0 Hz), 135.07, 131.13 (d, $J_{\text{C-F}} = 8.1$ Hz), 130.97, 128.41 (d, $J_{\text{C-F}} = 3.4$ Hz), 123.81, 123.05, 117.61 (dd, $J_{\text{C-F}} = 18.9$, 1.1 Hz), 115.9 (d, $J_{\text{C-F}} = 21.5$ Hz), 114.73, 112.32 (dd, $J_{\text{C-F}} = 6.0$, 3.8 Hz), 108.54, 106.7 (d, $J_{\text{C-F}} = 20.9$ Hz). ESI-HRMS (m/z): $[\text{M} - \text{H}]^-$ calcd for $\text{C}_{20}\text{H}_{10}\text{F}_3\text{O}_2\text{S}$, 371.0354; observed, 371.0346.

■ ASSOCIATED CONTENT

Supporting Information

The Supporting Information is available free of charge on the ACS Publications website at DOI: 10.1021/acs.jmedchem.5b01276.

X-ray crystallography verification for **29a** and effect of GPER antagonist, G15, on ShERPA luciferase activity (PDF)

Crystallographic data (CIF)

Molecular formula strings (CSV)

■ AUTHOR INFORMATION

Corresponding Author

*Phone: 312-355-5282. E-mail: thatcher@uic.edu.

Author Contributions

[†]R.X. and H.K.P. contributed equally.

The manuscript was written through contributions of all authors. All authors have given approval to the final version of the manuscript.

Notes

The authors declare no competing financial interest.

■ ACKNOWLEDGMENTS

This work was supported by NIH Grants R01 CA188017 and R01 CA102590, the University of Illinois Cancer Center, UIC Center for Clinical and Translational Science Grant UL1RR029879. We also thank Dr. Bernard D. Santarsiero from the Center for Pharmaceutical Biotechnology and the Department of Medicinal Chemistry and Pharmacognosy at UIC for his help with X-ray crystallography experiments.

■ ABBREVIATIONS USED

ShERPA, selective human estrogen receptor partial agonist; ER α , estrogen receptor α ; ER β , estrogen receptor β ; E $_2$, estradiol; SERM, selective estrogen receptor modulator; DES, diethylstilbestrol; LBD, ligand-binding domain; BPAF, bisphenol AF; PPA, polyphosphoric acid; FP, fluorescence polarization; ERE, estrogen response element; RBA $_{\text{rel}}$, relative binding affinity to raloxifene; RBA, relative binding affinity; SRC3, steroid receptor coregulator 3; AIB1, amplified in breast cancer 1; TR-FRET, time-resolved fluorescence (or Förster) resonance energy transfer; SEM, selective estrogen mimic; ChIP, chromatin immunoprecipitation; SA-Tb, streptavidin–terbium; CMC, carboxymethylcellulose; TLC, thin layer chromatography

■ REFERENCES

- (1) Deroo, B. J.; Korach, K. S. Estrogen receptors and human disease. *J. Clin. Invest.* **2006**, *116*, 561–570.
- (2) Sommer, S.; Fuqua, S. A. Estrogen receptor and breast cancer. *Semin. Cancer Biol.* **2001**, *11*, 339–352.
- (3) Jordan, V. C. Fourteenth Gaddum Memorial Lecture. A current view of tamoxifen for the treatment and prevention of breast cancer. *Br. J. Pharmacol.* **1993**, *110*, S07–S17.
- (4) Jordan, V. C. Tamoxifen: toxicities and drug resistance during the treatment and prevention of breast cancer. *Annu. Rev. Pharmacol. Toxicol.* **1995**, *35*, 195–211.
- (5) Ragaz, J.; Coldman, A. Survival impact of adjuvant tamoxifen on competing causes of mortality in breast cancer survivors, with analysis of mortality from contralateral breast cancer, cardiovascular events, endometrial cancer, and thromboembolic episodes. *J. Clin. Oncol.* **1998**, *16*, 2018–2024.
- (6) Ingle, J.; Ahmann, D.; Green, S.; Edmonson, J.; Bisel, H.; Kvols, L.; Nichols, W.; Creagan, E.; Hahn, R.; Rubin, J.; Frytak, S. Randomized clinical trial of diethylstilbestrol versus tamoxifen in postmenopausal women with advanced breast cancer. *N. Engl. J. Med.* **1981**, *304*, 16–21.
- (7) Ingle, J. N. Estrogen as therapy for breast cancer. *Breast Cancer Res.* **2002**, *4*, 133–136.
- (8) Schafer, J. M.; Lee, E. S.; Dardes, R. C.; Bentrem, D.; O'Regan, R. M.; De Los Reyes, A.; Jordan, V. C. Analysis of cross-resistance of the selective estrogen receptor modulators arzoxifene (LY353381) and LY117018 in tamoxifen-stimulated breast cancer xenografts. *Clin. Cancer Res.* **2001**, *7*, 2505–2512.
- (9) Roodi, N.; Bailey, L. R.; Kao, W. Y.; Verrier, C. S.; Yee, C. J.; Dupont, W. D.; Parl, F. F. Estrogen receptor gene analysis in estrogen

receptor-positive and receptor-negative primary breast cancer. *J. Natl. Cancer Inst.* **1995**, *87*, 446–451.

(10) Jordan, N. J.; Gee, J. M.; Barrow, D.; Wakeling, A. E.; Nicholson, R. I. Increased constitutive activity of PKB/Akt in tamoxifen resistant breast cancer MCF-7 cells. *Breast Cancer Res. Treat.* **2004**, *87*, 167–180.

(11) Schiff, R.; Massarweh, S. A.; Shou, J.; Bharwani, L.; Arpino, G.; Rimawi, M.; Osborne, C. K. Advanced concepts in estrogen receptor biology and breast cancer endocrine resistance: implicated role of growth factor signaling and estrogen receptor coregulators. *Cancer Chemother. Pharmacol.* **2005**, *56* (Suppl. 1), 10–20.

(12) Jordan, V. C.; Lewis, J. S.; Osipo, C.; Cheng, D. The apoptotic action of estrogen following exhaustive antihormonal therapy: A new clinical treatment strategy. *Breast* **2005**, *14*, 624–630.

(13) Craig Jordan, V.; Lewis-Wambi, J.; Kim, H.; Cunliffe, H.; Ariazi, E.; Sharma, C. G.; Shupp, H. A.; Swaby, R. Exploiting the apoptotic actions of oestrogen to reverse antihormonal drug resistance in oestrogen receptor positive breast cancer patients. *Breast* **2007**, *16*, S105–S113.

(14) Chalasani, P.; Stopeck, A.; Clarke, K.; Livingston, R. A pilot study of estradiol followed by exemestane for reversing endocrine resistance in postmenopausal women with hormone receptor-positive metastatic breast cancer. *Oncologist* **2014**, *19*, 1127–1128.

(15) Iwase, H.; Yamamoto, Y.; Yamamoto-Ibusuki, M.; Murakami, K. I.; Okumura, Y.; Tomita, S.; Inao, T.; Honda, Y.; Omoto, Y.; Iyama, K. I. Ethinylestradiol is beneficial for postmenopausal patients with heavily pre-treated metastatic breast cancer after prior aromatase inhibitor treatment: a prospective study. *Br. J. Cancer* **2013**, *109*, 1537–1542.

(16) Ellis, M. J.; Gao, F.; Dehdashti, F.; Jeffe, D. B.; Marcom, P. K.; Carey, L. A.; Dickler, M. N.; Silverman, P.; Fleming, G. F.; Kommareddy, A.; Jamalabadi-Majidi, S.; Crowder, R.; Siegel, B. A. Lower-dose vs high-dose oral estradiol therapy of hormone receptor-positive, aromatase inhibitor-resistant advanced breast cancer: a phase 2 randomized study. *JAMA* **2009**, *302*, 774–780.

(17) Carroll, J. S.; Liu, X. S.; Brodsky, A. S.; Li, W.; Meyer, C. A.; Szary, A. J.; Eeckhoutte, J.; Shao, W.; Hestermann, E. V.; Geistlinger, T. R.; Fox, E. A.; Silver, P. A.; Brown, M. Chromosome-wide mapping of estrogen receptor binding reveals long-range regulation requiring the forkhead protein FoxA1. *Cell* **2005**, *122*, 33–43.

(18) Merrell, K. W.; Crofts, J. D.; Smith, R. L.; Sin, J. H.; Kmetzsch, K. E.; Merrell, A.; Miguel, R. O.; Candelaria, N. R.; Lin, C. Y. Differential recruitment of nuclear receptor coregulators in ligand-dependent transcriptional repression by estrogen receptor- α . *Oncogene* **2011**, *30*, 1608–1614.

(19) Madak-Erdogan, Z.; Charn, T. H.; Jiang, Y.; Liu, E. T.; Katzenellenbogen, J. A.; Katzenellenbogen, B. S. Integrative genomics of gene and metabolic regulation by estrogen receptors α and β , and their coregulators. *Mol. Syst. Biol.* **2013**, *9*, 676.

(20) Maximov, P. Y.; Lee, T. M.; Jordan, V. C. The Discovery and Development of Selective Estrogen Receptor Modulators (SERMs) for Clinical Practice. *Curr. Clin. Pharmacol.* **2013**, *8*, 135–155.

(21) Sporn, M. B. Arzoxifene: a promising new selective estrogen receptor modulator for clinical chemoprevention of breast cancer. *Clin. Cancer Res.* **2004**, *10*, S313–S315.

(22) Baselga, J.; Llombart-Cussac, A.; Bellet, M.; Guillem-Porta, V.; Enas, N.; Krejcy, K.; Carrasco, E.; Kayitalire, L.; Kuta, M.; Lluch, A.; Vodvarka, P.; Kerbrat, P.; Namer, M.; Petruzella, L. Randomized, double-blind, multicenter trial comparing two doses of arzoxifene (LY353381) in hormone-sensitive advanced or metastatic breast cancer patients. *Ann. Oncol.* **2003**, *14*, 1383–1390.

(23) Chan, S. Arzoxifene in breast cancer. *Eur. J. Cancer* **2002**, *38* (Suppl. 6), S55–S56.

(24) Dardes, R. C.; Bentrem, D.; O'Regan, R. M.; Schafer, J. M.; Jordan, V. C. Effects of the new selective estrogen receptor modulator LY353381.HCl (Arzoxifene) on human endometrial cancer growth in athymic mice. *Clin. Cancer Res.* **2001**, *7*, 4149–4155.

(25) McMeekin, D. S.; Gordon, A.; Fowler, J.; Melemed, A.; Buller, R.; Burke, T.; Bloss, J.; Sabbatini, P. A phase II trial of arzoxifene, a selective estrogen response modulator, in patients with recurrent or advanced endometrial cancer. *Gynecol. Oncol.* **2003**, *90*, 64–69.

(26) Suh, N.; Glasebrook, A. L.; Palkowitz, A. D.; Bryant, H. U.; Burris, L. L.; Starling, J. J.; Pearce, H. L.; Williams, C.; Peer, C.; Wang, Y.; Sporn, M. B. Arzoxifene, a new selective estrogen receptor modulator for chemoprevention of experimental breast cancer. *Cancer Res.* **2001**, *61*, 8412–8415.

(27) Taylor, H. S. Approaching the ideal selective estrogen receptor modulator for prevention and treatment of postmenopausal osteoporosis. *Formulary* **2010**, *45*, 52–61.

(28) Pickar, J. H. The endometrium - from estrogens alone to TSEC's. *Climacteric* **2009**, *12*, 463–477.

(29) Lobo, R. A.; et al. Evaluation of bazedoxifene/conjugated estrogens for the treatment of menopausal symptoms and effects on metabolic parameters and overall safety profile. *Fertil. Steril.* **2009**, *92*, 1025–1038.

(30) Toader, V.; Xu, X.; Nicolescu, A.; Yu, L.; Bolton, J. L.; Thatcher, G. R. J. Nitrosation, nitration, and autooxidation of the selective estrogen receptor modulator raloxifene by nitric oxide, peroxyxynitrite, and reactive nitrogen/oxygen species. *Chem. Res. Toxicol.* **2003**, *16*, 1264–1276.

(31) Liu, J.; Li, Q.; Yang, X.; van Breemen, R. B.; Bolton, J. L.; Thatcher, G. R. J. Analysis of protein covalent modification by xenobiotics using a covert oxidatively activated tag: raloxifene proof-of-principle study. *Chem. Res. Toxicol.* **2005**, *18*, 1485–1496.

(32) Liu, H.; Liu, J.; van Breemen, R. B.; Thatcher, G. R. J.; Bolton, J. L. Bioactivation of the selective estrogen receptor modulator desmethylated arzoxifene to quinoids: 4'-fluoro substitution prevents quinoid formation. *Chem. Res. Toxicol.* **2005**, *18*, 162–173.

(33) Bolton, J. L.; Yu, L.; Thatcher, G. R. J. Quinoids formed from estrogens and antiestrogens. *Methods Enzymol.* **2004**, *378*, 110–123.

(34) Liu, H.; Bolton, J. L.; Thatcher, G. R. J. Chemical modification modulates estrogenic activity, oxidative reactivity, and metabolic stability in 4'-F-DMA, a new benzothiophene selective estrogen receptor modulator. *Chem. Res. Toxicol.* **2006**, *19*, 779–787.

(35) Yu, B.; Dietz, B. M.; Dunlap, T.; Kastrati, I.; Lantvit, D. D.; Overk, C. R.; Yao, P.; Qin, Z.; Bolton, J. L.; Thatcher, G. R. J. Structural modulation of reactivity/activity in design of improved benzothiophene selective estrogen receptor modulators: induction of chemopreventive mechanisms. *Mol. Cancer Ther.* **2007**, *6*, 2418–2428.

(36) Overk, C. R.; Peng, K. W.; Asghodom, R. T.; Kastrati, I.; Lantvit, D. D.; Qin, Z.; Frasier, J.; Bolton, J. L.; Thatcher, G. R. J. Structure-activity relationships for a family of benzothiophene selective estrogen receptor modulators including raloxifene and arzoxifene. *ChemMedChem* **2007**, *2*, 1520–1526.

(37) Liu, H.; Qin, Z.; Thatcher, G. R. J.; Bolton, J. L. Uterine peroxidase-catalyzed formation of diquinone methides from the selective estrogen receptor modulators raloxifene and desmethylated arzoxifene. *Chem. Res. Toxicol.* **2007**, *20*, 1676–1684.

(38) Qin, Z.; Kastrati, I.; Ashgodom, R. T.; Lantvit, D. D.; Overk, C. R.; Choi, Y.; van Breemen, R. B.; Bolton, J. L.; Thatcher, G. R. J. Structural modulation of oxidative metabolism in design of improved benzothiophene selective estrogen receptor modulators. *Drug Metab. Dispos.* **2009**, *37*, 161–169.

(39) Kastrati, I.; Edirisinghe, P. D.; Hemachandra, L. P.; Chandrasena, E. R.; Choi, J.; Wang, Y. T.; Bolton, J. L.; Thatcher, G. R. Raloxifene and desmethylaraloxifene block estrogen-induced malignant transformation of human breast epithelial cells. *PLoS One* **2011**, *6*, e27876.

(40) Patel, H. K.; Siklos, M. I.; Abdelkarim, H.; Mendonca, E. L.; Vaidya, A.; Petukhov, P. A.; Thatcher, G. R. A chimeric SERM-Histone deacetylase inhibitor approach to breast cancer therapy. *ChemMedChem* **2014**, *9*, 602–613.

(41) Hemachandra, L. P.; Patel, H.; Chandrasena, R. E.; Choi, J.; Piyankarage, S. C.; Wang, S.; Wang, Y.; Thayer, E. N.; Scism, R. A.; Michalsen, B. T.; Xiong, R.; Siklos, M. I.; Bolton, J. L.; Thatcher, G. R. SERMs attenuate estrogen-induced malignant transformation of human mammary epithelial cells by upregulating detoxification of oxidative metabolites. *Cancer Prev. Res.* **2014**, *7*, S05–S15.

(42) Molloy, M. E.; White, B. E.; Gherezghiher, T.; Michalsen, B. T.; Xiong, R.; Patel, H.; Zhao, H.; Maximov, P. Y.; Jordan, V. C.; Thatcher, G. R.; Tonetti, D. A. Novel selective estrogen mimics for the treatment

of tamoxifen-resistant breast cancer. *Mol. Cancer Ther.* **2014**, *13*, 2515–2526.

(43) Katzenellenbogen, J. A. The 2010 Philip S. Portoghesi Medicinal Chemistry Lectureship: addressing the "core issue" in the design of estrogen receptor ligands. *J. Med. Chem.* **2011**, *54*, 5271–5282.

(44) Anstead, G. M.; Carlson, K. E.; Katzenellenbogen, J. A. The estradiol pharmacophore: ligand structure-estrogen receptor binding affinity relationships and a model for the receptor binding site. *Steroids* **1997**, *62*, 268–303.

(45) Nettles, K. W.; Bruning, J. B.; Gil, G.; O'Neill, E. E.; Nowak, J.; Guo, Y.; Kim, Y.; DeSombre, E. R.; Dilis, R.; Hanson, R. N.; Joachimiak, A.; Greene, G. L. Structural plasticity in the oestrogen receptor ligand-binding domain. *EMBO Rep.* **2007**, *8*, 563–568.

(46) Brzozowski, A. M.; Pike, A. C.; Dauter, Z.; Hubbard, R. E.; Bonn, T.; Engstrom, O.; Ohman, L.; Greene, G. L.; Gustafsson, J. A.; Carlquist, M. Molecular basis of agonism and antagonism in the oestrogen receptor. *Nature* **1997**, *389*, 753–758.

(47) Dang, Z. C.; Audinot, V.; Papapoulos, S. E.; Boutin, J. A.; Lowik, C. W. Peroxisome proliferator-activated receptor gamma (PPARgamma) as a molecular target for the soy phytoestrogen genistein. *J. Biol. Chem.* **2003**, *278*, 962–967.

(48) Hsieh, C. Y.; Santell, R. C.; Haslam, S. Z.; Helferich, W. G. Estrogenic effects of genistein on the growth of estrogen receptor-positive human breast cancer (MCF-7) cells in vitro and in vivo. *Cancer Res.* **1998**, *58*, 3833–3838.

(49) Rao, A.; Coan, A.; Welsh, J. E.; Barclay, W. W.; Koumenis, C.; Cramer, S. D. Vitamin D receptor and p21/WAF1 are targets of genistein and 1,25-dihydroxyvitamin D3 in human prostate cancer cells. *Cancer Res.* **2004**, *64*, 2143–2147.

(50) Min, J.; Wang, P.; Srinivasan, S.; Nwachukwu, J. C.; Guo, P.; Huang, M.; Carlson, K. E.; Katzenellenbogen, J. A.; Nettles, K. W.; Zhou, H. B. Thiophene-core estrogen receptor ligands having superagonist activity. *J. Med. Chem.* **2013**, *56*, 3346–3366.

(51) Wang, P.; Min, J.; Nwachukwu, J. C.; Cavett, V.; Carlson, K. E.; Guo, P.; Zhu, M.; Zheng, Y.; Dong, C.; Katzenellenbogen, J. A.; Nettles, K. W.; Zhou, H. B. Identification and structure-activity relationships of a novel series of estrogen receptor ligands based on 7-thiabicyclo[2.2.1]hept-2-ene-7-oxide. *J. Med. Chem.* **2012**, *55*, 2324–2341.

(52) Minutolo, F.; Bellini, R.; Bertini, S.; Carboni, I.; Lapucci, A.; Pistolesi, L.; Protta, G.; Rapposelli, S.; Solati, F.; Tuccinardi, T.; Martinelli, A.; Stossi, F.; Carlson, K. E.; Katzenellenbogen, B. S.; Katzenellenbogen, J. A.; Macchia, M. Monoaryl-substituted salicylaldoximes as ligands for estrogen receptor beta. *J. Med. Chem.* **2008**, *51*, 1344–1351.

(53) Hanson, R. N.; Hua, E.; Hendricks, J. A.; Labaree, D.; Hochberg, R. B. Synthesis and evaluation of 11beta-(4-substituted phenyl) estradiol analogs: transition from estrogen receptor agonists to antagonists. *Bioorg. Med. Chem.* **2012**, *20*, 3768–3780.

(54) Delfosse, V.; Grimaldi, M.; Pons, J. L.; Boulahtouf, A.; le Maire, A.; Cavailles, V.; Labesse, G.; Bourguet, W.; Balaguer, P. Structural and mechanistic insights into bisphenols action provide guidelines for risk assessment and discovery of bisphenol A substitutes. *Proc. Natl. Acad. Sci. U. S. A.* **2012**, *109*, 14930–14935.

(55) Steffan, R. J.; Matelan, E.; Ashwell, M. A.; Moore, W. J.; Solvibile, W. R.; Trybulski, E.; Chadwick, C. C.; Chippari, S.; Kenney, T.; Eckert, A.; Borges-Marcucci, L.; Keith, J. C.; Xu, Z.; Mosyak, L.; Harnish, D. C. Synthesis and activity of substituted 4-(indazol-2-yl)phenols as pathway-selective estrogen receptor ligands useful in the treatment of rheumatoid arthritis. *J. Med. Chem.* **2004**, *47*, 6435–6438.

(56) Bruning, J. B.; Parent, A. A.; Gil, G.; Zhao, M.; Nowak, J.; Pace, M. C.; Smith, C. L.; Afonine, P. V.; Adams, P. D.; Katzenellenbogen, J. A.; Nettles, K. W. Coupling of receptor conformation and ligand orientation determine graded activity. *Nat. Chem. Biol.* **2010**, *6*, 837–843.

(57) Jones, C. D.; Jevnikar, M. G.; Pike, A. J.; Peters, M. K.; Black, L. J.; Thompson, A. R.; Falcone, J. F.; Clemens, J. A. Antiestrogens 0.2. Structure Activity Studies in a Series of 3-Aroyl-2-Arylbenzo[B]-Thiophene Derivatives Leading to [6-Hydroxy-2-(4-Hydroxyphenyl)-Benzo[B]Thien-3-Yl][4-[2-(1-Piperidinyl)Ethoxy]-Phenyl]-

Methanone Hydrochloride (Ly156758), a Remarkably Effective Estrogen Antagonist with Only Minimal Intrinsic Estrogenicity. *J. Med. Chem.* **1984**, *27*, 1057–1066.

(58) Hillver, S. E.; Bjork, L.; Li, Y. L.; Svensson, B.; Ross, S.; Anden, N. E.; Hacksell, U. (S)-5-fluoro-8-hydroxy-2-(dipropylamino)tetralin: a putative 5-HT1A-receptor antagonist. *J. Med. Chem.* **1990**, *33*, 1541–1544.

(59) Krapcho, A. P.; Menta, E.; Oliva, A.; Di Domenico, R.; Fiocchi, L.; Maresch, M. E.; Gallagher, C. E.; Hacker, M. P.; Beggiolin, G.; Giuliani, F. C.; Pezzoni, G.; Spinelli, S. Synthesis and antitumor evaluation of 2,5-disubstituted-indazolo[4, 3-gh]isoquinolin-6(2H)-ones (9-aza-anthra-pyrazoles). *J. Med. Chem.* **1998**, *41*, 5429–5444.

(60) Liu, X. F.; Bagchi, M. K. Recruitment of distinct chromatin-modifying complexes by tamoxifen-complexed estrogen receptor at natural target gene promoters in vivo. *J. Biol. Chem.* **2004**, *279*, 15050–15058.

(61) Hayakawa, T.; Nakayama, J. Physiological roles of class I HDAC complex and histone demethylase. *J. Biomed. Biotechnol.* **2011**, *2011*, 129383.

(62) Fischle, W.; Dequiedt, F.; Hendzel, M. J.; Guenther, M. G.; Lazar, M. A.; Voelter, W.; Verdin, E. Enzymatic activity associated with class II HDACs is dependent on a multiprotein complex containing HDAC3 and SMRT/N-CoR. *Mol. Cell* **2002**, *9*, 45–57.

(63) Onate, S. A.; Tsai, S. Y.; Tsai, M. J.; Omalley, B. W. Sequence and Characterization of a Coactivator for the Steroid-Hormone Receptor Superfamily. *Science* **1995**, *270*, 1354–1357.

(64) Anzick, S. L.; Kononen, J.; Walker, R. L.; Azorsa, D. O.; Tanner, M. M.; Guan, X. Y.; Sauter, G.; Kallioniemi, O. P.; Trent, J. M.; Meltzer, P. S. AIB1, a steroid receptor coactivator amplified in breast and ovarian cancer. *Science* **1997**, *277*, 965–968.

(65) Gunther, J. R.; Du, Y. H.; Rhoden, E.; Lewis, I.; Revennaugh, B.; Moore, T. W.; Kim, S. H.; Dingleline, R.; Fu, H. A.; Katzenellenbogen, J. A. A Set of Time-Resolved Fluorescence Resonance Energy Transfer Assays for the Discovery of Inhibitors of Estrogen Receptor-Coactivator Binding. *J. Biomol. Screening* **2009**, *14*, 181–193.

(66) Jayakumar, M.; Carlson, K. E.; Gunther, J. R.; Katzenellenbogen, J. A. Exploration of dimensions of estrogen potency: parsing ligand binding and coactivator binding affinities. *J. Biol. Chem.* **2011**, *286*, 12971–12982.

(67) Ariazi, E. A.; Cunliffe, H. E.; Lewis-Wambi, J. S.; Slifker, M. J.; Willis, A. L.; Ramos, P.; Tapia, C.; Kim, H. R.; Yerrum, S.; Sharma, C. G.; Nicolas, E.; Balagurunathan, Y.; Ross, E. A.; Jordan, V. C. Estrogen induces apoptosis in estrogen deprivation-resistant breast cancer through stress responses as identified by global gene expression across time. *Proc. Natl. Acad. Sci. U. S. A.* **2011**, *108*, 18879–18886.

(68) Tonetti, D. A.; Chisamore, M. J.; Grdina, W.; Schurz, H.; Jordan, V. C. Stable transfection of protein kinase C alpha cDNA in hormone-dependent breast cancer cell lines. *Br. J. Cancer* **2000**, *83*, 782–791.

(69) Jordan, V. C.; Lewis-Wambi, J. S.; Patel, R. R.; Kim, H.; Ariazi, E. A. New hypotheses and opportunities in endocrine therapy: amplification of oestrogen-induced apoptosis. *Breast* **2009**, *18*, S10–S17.

(70) Lewis-Wambi, J. S.; Jordan, V. C. Estrogen regulation of apoptosis: how can one hormone stimulate and inhibit? *Breast Cancer Res.* **2009**, *11*, 206.

(71) Grese, T. A.; Cho, S.; Finley, D. R.; Godfrey, A. G.; Jones, C. D.; Lugar, C. W., 3rd; Martin, M. J.; Matsumoto, K.; Pennington, L. D.; Winter, M. A.; Adrian, M. D.; Cole, H. W.; Magee, D. E.; Phillips, D. L.; Rowley, E. R.; Short, L. L.; Glasebrook, A. L.; Bryant, H. U. Structure-activity relationships of selective estrogen receptor modulators: modifications to the 2-arylbenzothiophene core of raloxifene. *J. Med. Chem.* **1997**, *40*, 146–167.

(72) Dutertre, M.; Smith, C. L. Molecular mechanisms of selective estrogen receptor modulator (SERM) action. *J. Pharmacol. Exp. Ther.* **2000**, *295*, 431–437.

(73) Johnson, A. B.; O'Malley, B. W. Steroid receptor coactivators 1, 2, and 3: critical regulators of nuclear receptor activity and steroid receptor modulator (SRM)-based cancer therapy. *Mol. Cell. Endocrinol.* **2012**, *348*, 430–439.

(74) Dai, S. Y.; Burris, T. P.; Dodge, J. A.; Montrose-Rafizadeh, C.; Wang, Y.; Pascal, B. D.; Chalmers, M. J.; Griffin, P. R. Unique ligand binding patterns between estrogen receptor alpha and beta revealed by hydrogen-deuterium exchange. *Biochemistry* **2009**, *48*, 9668–9676.

(75) Katzenellenbogen, J. A.; Johnson, H. J., Jr.; Myers, H. N. Photoaffinity labels for estrogen binding proteins of rat uterus. *Biochemistry* **1973**, *12*, 4085–4092.

(76) Carlson, K. E.; Choi, I.; Gee, A.; Katzenellenbogen, B. S.; Katzenellenbogen, J. A. Altered ligand binding properties and enhanced stability of a constitutively active estrogen receptor: evidence that an open pocket conformation is required for ligand interaction. *Biochemistry* **1997**, *36*, 14897–14905.

(77) Chisamore, M. J.; Ahmed, Y.; Bentrem, D. J.; Jordan, V. C.; Tonetti, D. A. Novel antitumor effect of estradiol in athymic mice injected with a T47D breast cancer cell line overexpressing protein kinase Calpha. *Clin. Cancer Res.* **2001**, *7*, 3156–3165.